BASS

Bolometer Array Survey Spectrograph

For SPICA

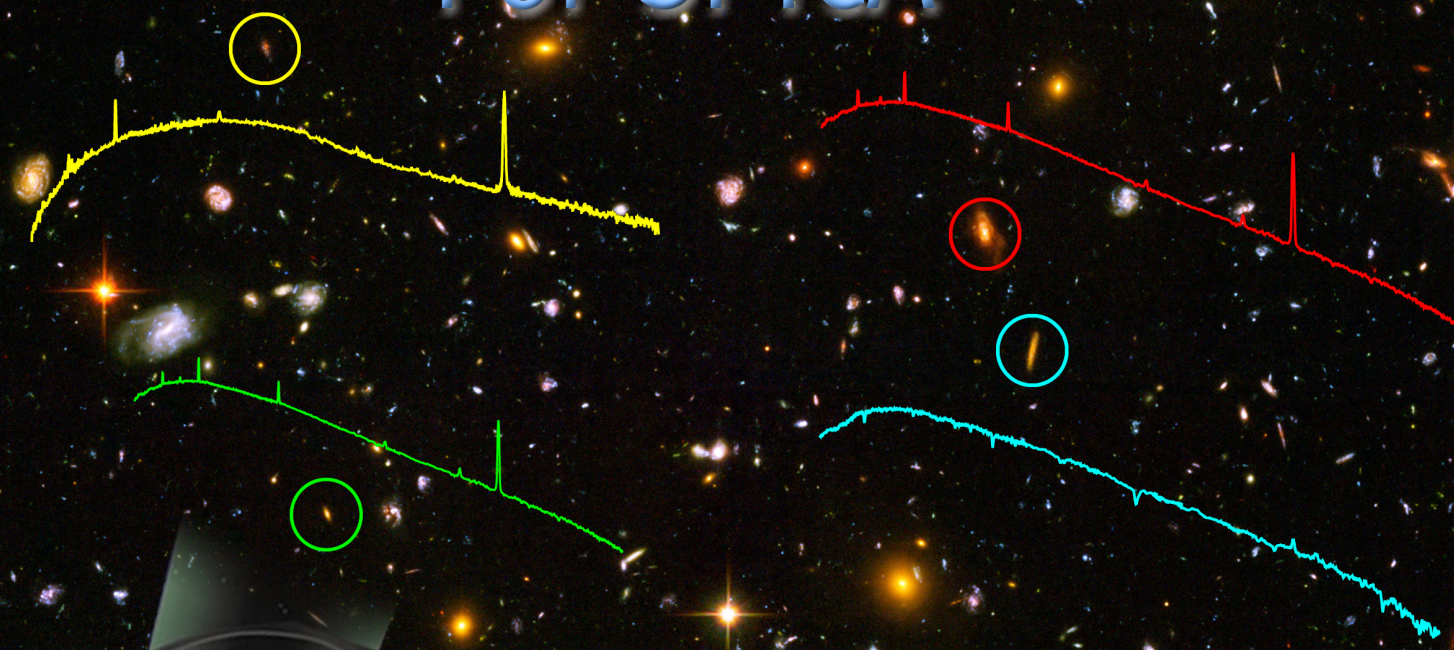

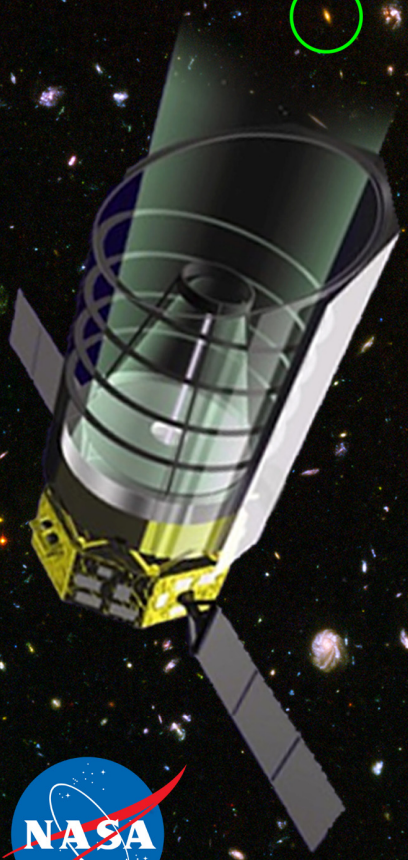

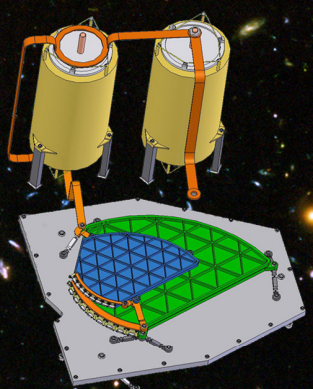

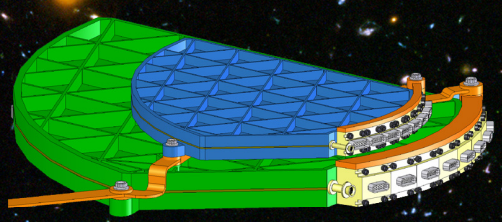

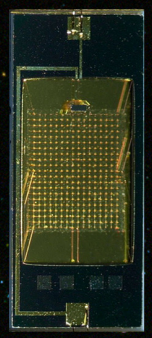

NASA JAXA JPL

Cover: Hubble Ultra Deep Field with ISO Long Wavelength Spectrometer (LWS) spectra of nearby galaxies (Fischer et al., 1999). The spectra extend from 48 to 200 microns, a range covered by BASS for redshift ~ 1, and BASS-SPICA will readily obtain spectra of galaxies in this epoch. The circles show the BASS Band A beamsize.

Background image credit: NASA, ESA, S. Beckwith (SCSCI) and the HUDF team.

BASS for SPICA
Revealing the History of Energy Production in Galaxies

The Bolometer Array Survey Spectrograph (BASS) is a sensitive far-IR/submm spectrograph for the Japanese-led SPace Infrared telescope for Cosmology and Astrophysics (SPICA) mission. With its 3.5-meter actively-cooled telescope, SPICA will be the world's premier platform for far-IR astronomical observations at the end of the next decade. BASS is a mission of opportunity that employs unique US far-IR focal-plane technologies and will open the early universe to far-IR spectroscopy for the first time. With BASS spectra, we will chart the history of dust-obscured stars, black holes, and the elements of life through cosmic time. BASS will also serve as an entry point for U.S. astronomers to participate in the greater SPICA mission.

A Cold Telescope Enables Sensitive Far-IR - Submm Spectroscopy

- Herschel, SOFIA and ground based platforms are limited by photon noise from their warm telescopes.
- The ultimate limitation is the astrophysical backgrounds with ~1000 times lower noise.
- A cryogenic telescope enables **spectroscopy at z=1-5**

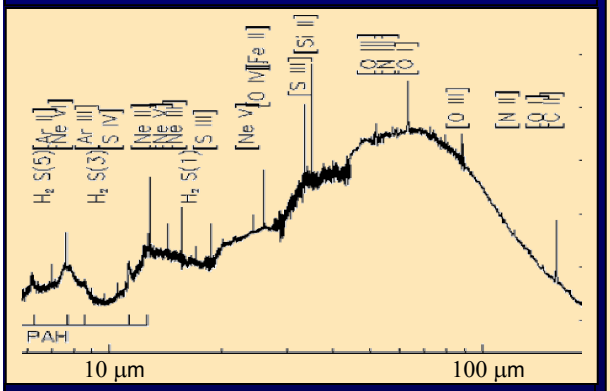

- **Far-IR spectroscopy is immune to dust extinction.**
- **Galaxy spectra reveal the hidden processes which produced the modern universe:**

* buildup of stars and organic elements.
* embedded accretion and black hole growth.

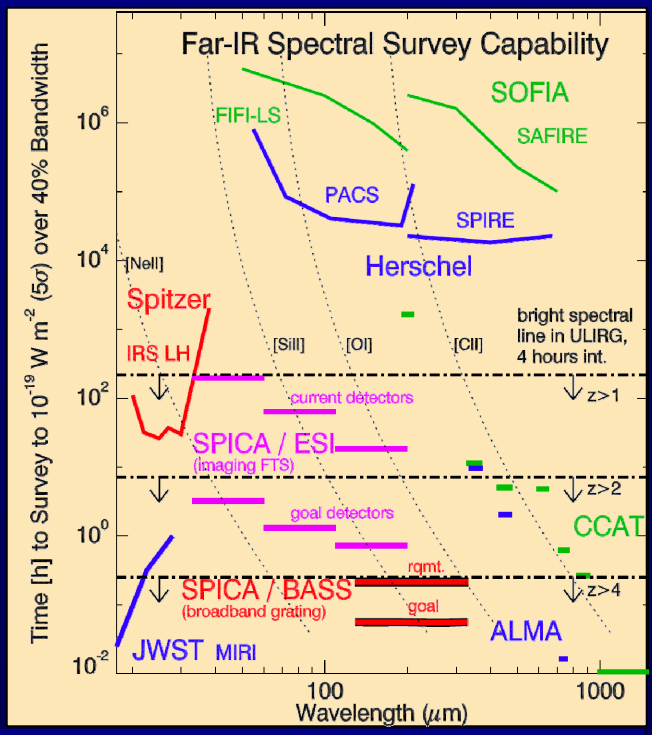

BASS Team

Science Direction, Hardware (PI, co-Is, management)	
Matt Bradford (JPL, Caltech)	BASS PI: Instrument design, overall quality of science products
James Bock (JPL, Caltech)	BASS co-I & instrument scientist
Alfred Nash (JPL)	BASS project manager
Warren Holmes (JPL)	BASS co-I & sub-K cooler lead
Timothy Koch (JPL)	BASS systems engineering manager
Hideo Matsuhara (ISAS/JAXA)	BASS co-I & SPICA liaison
Scientific Software / Archiving (co-Is)	
George Helou (IPAC, Caltech)	Data archiving, IPAC interface
Lee Armus (IPAC, Caltech)	Spectral calibration, data pipelining
JD Smith (Toledo)	Reduction and analysis software

Scientific Oversight (co-Is)	
Takao Nakagawa (ISAS/JAXA)	SPICA PI: Direction of SPICA mission and approval of BASS role.
Scott Chapman (Cambridge)	Galaxy population modeling
Uma Gorti (Berkeley)	Protoplanetary disk modeling
Martin Harwit (Cornell)	Molecular gas cooling, international experience with Herschel
Dan Lester (Texas)	Abundance measurements, SAFIR liaison
Matt Malkan (UCLA)	Active galactic nuclei (AGN)
George Rieke (Arizona)	Galaxy sample selection, MIPS experience for JWST liaison
Gordon Stacey (Cornell)	Atomic and ionized gas cooling
Michael Werner (JPL)	Spitzer experience for development

SPICA Mission Overview

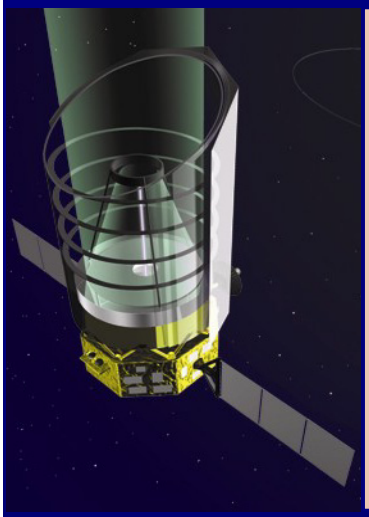

Launch: ~ 2017
Lifetime: 5 years
Orbit: L2 Halo
Aperture: 3.5 m dia.
Temperatue: **4.5 K** with cryocoolers
Programmatic Style:
Great Observatory with key projects, legacy science teams, international participation
International Partners:
Japan, Europe, Korea
Timescale:
Phase A ~ 2008–2009
Instrument Selection ~ 2009–2010

BASS Detectors
enabling sensitive spectroscopy with proven heritage

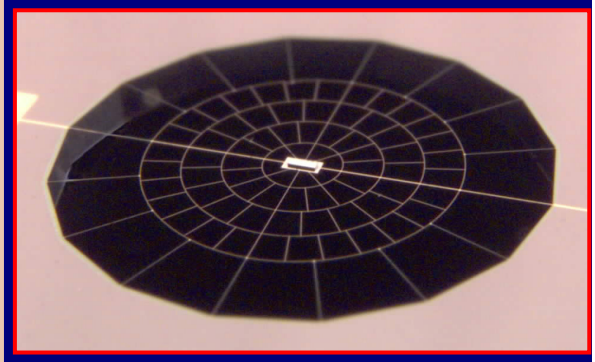

JPL-built micro-mesh bolometers with JFET readouts. Delivered for Herschel and Planck, well characterized, reliable, TRL 8–9. **Proposed here for BASS.**

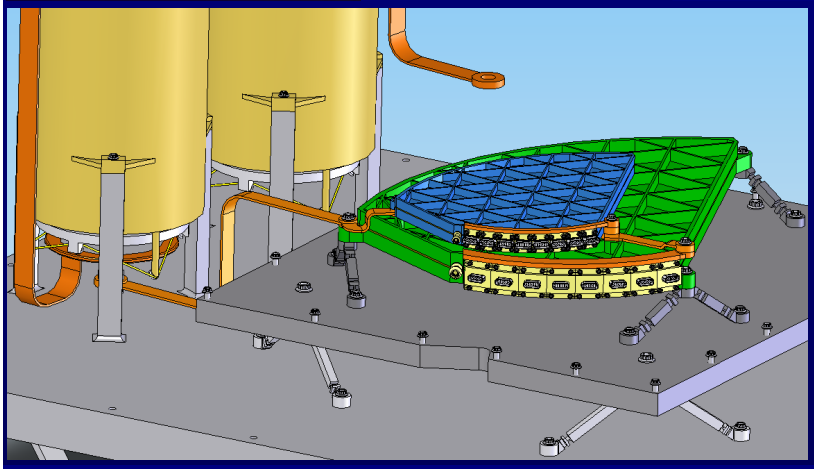

BASS Instrument Concept

Two waveguide spectrometer modules.
A: 132-210 μm, B: 210-340 μm

Resolving power: 300

Chopping mirror modulates source between the two spectrometers—the only moving part.

Adiabatic Demagnetization Refrigerator (ADR) cools gratings and detectors to 50 mK, interfaces with 1.7 K spacecraft cooler.

Modest interfaces: Mass: <40 kg, Power: <50 W, Heat lift required at 1.7K: <5 mW

Management

BASS will be built and managed by the Jet Propulsion Laboratory. The PI mission cost for BASS is $70M (FY08$). An 18-month, $5.3M (FY08$) advanced development phase is included prior to the 36-month flight development phase to retire risks with detectors, cryocooler, readout electronics and the SPICA thermal interfaces. Although SMEX calls for a class D mission, our BASS costs were developed consistent with class B requirements anticipated from SPICA. BASS is scheduled for delivery in June 2013, allowing more than 2 years of schedule reserve for integration with SPICA.

Cost/Schedule

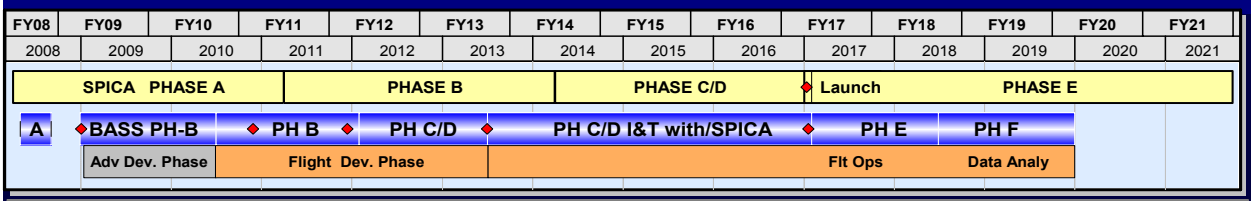

WBS Element	Phase A RY $K	Phase B RY $K	Phase C/D RY $K	Phase E RY $K	Phase F RY $K	Total (A–F) RY $K	Total (A–F) FY08 $K
Advanced Dev. Phase		5,598				5,598	5,343
BASS Instrument	250	11,423	37,897	287	0	49,858	44,535
Science		239	1,137	1,698	1,740	4,814	3,619
Reserves		1,166	16,394	596	522	18,678	16,372
PI Mission Cost	250	18,426	55,428	2,581	2,262	78,948	69,868

C. TABLE OF CONTENTS

D. SCIENCE INVESTIGATION

D.1 Overview

We propose to use world-leading NASA technology to build a sensitive spectrograph for the premier far-IR astronomical observatory of the next decade. The Japanese-led Space Infrared Telescope for Cosmology and Astrophysics (SPICA) mission is a 3.5-meter telescope actively cooled to below 5 K, and is planned for launch to an Earth-Sun L2-point orbit in 2017. Our team has been collaborating with SPICA Principal Investigator (PI) Takao Nakagawa and his team, and have developed a bolometer-based spectrograph BASS (bolometer array survey spectrograph) as a mission of opportunity. BASS will both enhance the scientific output of SPICA and serve as an entry point for U.S. scientists to participate in the full astronomical capabilities of the mission. The collaboration is compelling because BASS incorporates very sensitive, far-IR–submillimeter detector arrays for which the U.S. is the world leader.

The combination of SPICA's large cold telescope and the excellent sensitivity of BASS will make for a powerful new probe of the dust-enshrouded universe. BASS will cover the 132–340 μm range, and with the cold SPICA telescope will offer 4 orders of magnitude improvement in speed over planned facilities for spectroscopy. BASS, along with the proposed European SPICA Instrument (ESI) operating at shorter wavelengths, will provide the first platform for high-redshift spectroscopy in the far-IR waveband where many galaxies emit the bulk of their power.

The BASS core science program will use approximately 1000 hours of SPICA time with BASS to obtain spectra of 500 galaxies ranging from the local universe to redshift 4. **In aggregate, this core set of galaxy spectra will chart the history of stars, black hole activity, and organic element production from 2 GY after the Big Bang to the present.**

A NASA contribution to SPICA will provide U.S. scientists access to the full capabilities of the flagship-class observatory at a fraction of the mission's full cost. SPICA is currently the only space-borne far-IR facility with capability longward of 28 μm planned for the 2015–2020 epoch. It will provide wavelength coverage and sensitivity necessary to complement JWST and ALMA, multiplying the returns from all three missions. By providing BASS for SPICA, the U.S. astronomical community will be engaged in all aspects of the resulting opportunities for breakthroughs and discoveries. BASS will also provide the platform for advancing low-background far-IR focal-plane technologies after Herschel but before the U.S.-led cryogenic far-IR missions such as CALISTO/SAFIR and SPIRIT/SPECs.

D.1.1 The SPICA Vision: The World's First Large Cold Telescope

The far-IR spectral regime is the repository of half the electromagnetic energy released in the history of stars and galaxies, and offers the only opportunity to probe many of the most pressing questions in modern astrophysics. Yet compared with other wavebands, the far-IR has remained a relatively unexplored frontier because sensitive far-IR measurements require a combination that has yet to be fully realized: a large cryogenic telescope above the atmosphere using sensitive far-IR focal-plane technologies. The multi-national SPICA team is now poised to build on the experience with IRAS, ISO, Spitzer, Akari, and Herschel to provide these capabilities.

The most important attribute of SPICA is its sub-5 K temperature. To understand the impact of this, consider that at 100 μm, even a well-designed passively-cooled T~80 K telescope such as Herschel is 10,000 to 100,000 times brighter than the natural astrophysical background due to solar-system and Galactic dust. Cooling the telescope to below 5 K virtually eliminates its emission relative to these backgrounds. The sensitivity improvement afforded by a cold telescope can be dramatic, as resoundingly demonstrated with Spitzer's successes in the mid- and far-infrared. SPICA is conceived in this same philosophy, and JAXA has invested significantly over the past 5 years to develop and verify closed-cycle 4-K and 2-K cryocoolers to enable the 5-year mission. SPICA's large, cold aperture combined with BASS will directly address two of the four targeted questions in NASA's 2007 Science Plan: **How do Planets, Stars, Galaxies and Cosmic Structures Come Into Being?** and **When and How Did the Elements of Life in the Universe Arise?**

JAXA's key goals for the SPICA mission are similar: 1) The birth and evolution of galaxies, 2) the chemical evolution of the Universe, and 3) the birth and evolution of stars and planets.

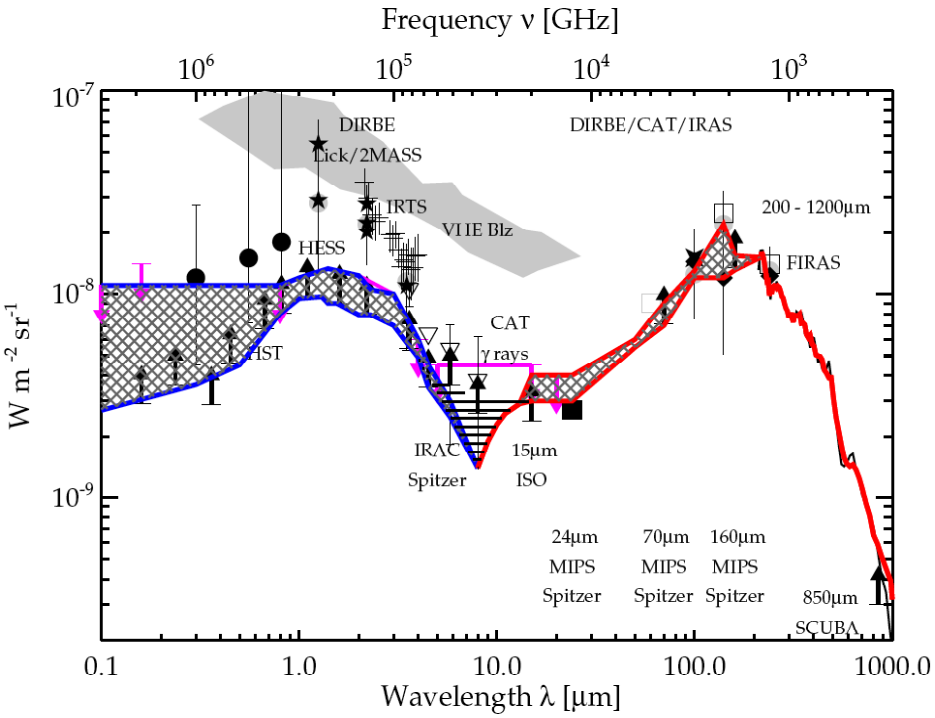

Figure D-1. *Observational constraints on the intensity of the cosmic background radiation from radio to ultraviolet wavelengths, reprinted from Dole et al. (2006). The two peaks, one in the optical/near-IR and one in the far-IR, have comparable energy density. This implies that half of the energy released throughout the history of stars and galaxies is absorbed by dust.*

These topics require far-IR measurements because young stars and black holes are often hidden in clouds of dust. Indeed, from our view of the Universe, half the total energy from all stars and galaxies has been absorbed and re-radiated in the far-IR (**Figures D-1** and **D-2**). This phenomenon occurs on all scales, from individual star-formation sites to entire galaxies and active nuclei, for which up to 99% of the optical radiation is absorbed by the dust and emerges in the far-IR. The peak of the CIB, near 140 μm suggests a typical redshift $z\sim1$, but the long-wavelength tail of the CIB exceeds the flux expected from the sources that generated the peak, indicating dust-obscured activity at even higher redshifts. It is clear that mid-and far-IR measurements are required for understanding how the present-day Universe came to be.

D.1.2 Open-Time Science with SPICA

The details of the observing allocation for SPICA will be worked out in SPICA's Phase-A study, but it is anticipated that U.S. scientists will have access to SPICA's open time in exchange for the provision of BASS (see attached letter from SPICA PI Takao Nakagawa). The open time will likely solicit proposals for large legacy as well as general observer programs as has proven successful on the U.S. great observatories and is being implemented with Herschel. SPICA will have a powerful suite of mid- and far-IR instruments outlined in **Table D-1**. While we can not provide a complete compilation, we highlight just a few of SPICA's most exciting scientific prospects which could be available to U.S. scientists in open time observations (see also **Foldout 2 [FO2]**):

1) The birth of planetary systems. SPICA offers unique capabilities to probe all phases of the planet-formation process, from early gas-rich protostars to debris disks with very little remaining gas and dust. Sensitivity to small far-IR dust excesses will identify candidate protostar/disk sources within a few hundred pc. They can then be followed up with high-resolution ($R\sim10{,}000$-$30{,}000$) spectroscopy in the mid- and far-IR to reveal infalling and out-flowing gas. Complete spectral coverage into the sub-millimeter with ESI and BASS will measure the gas mass, and identify its constituents, including pre-biotic materials if they are present.

2) Direct imaging of planets with an advanced mid-IR coronagraph. With SPICA's

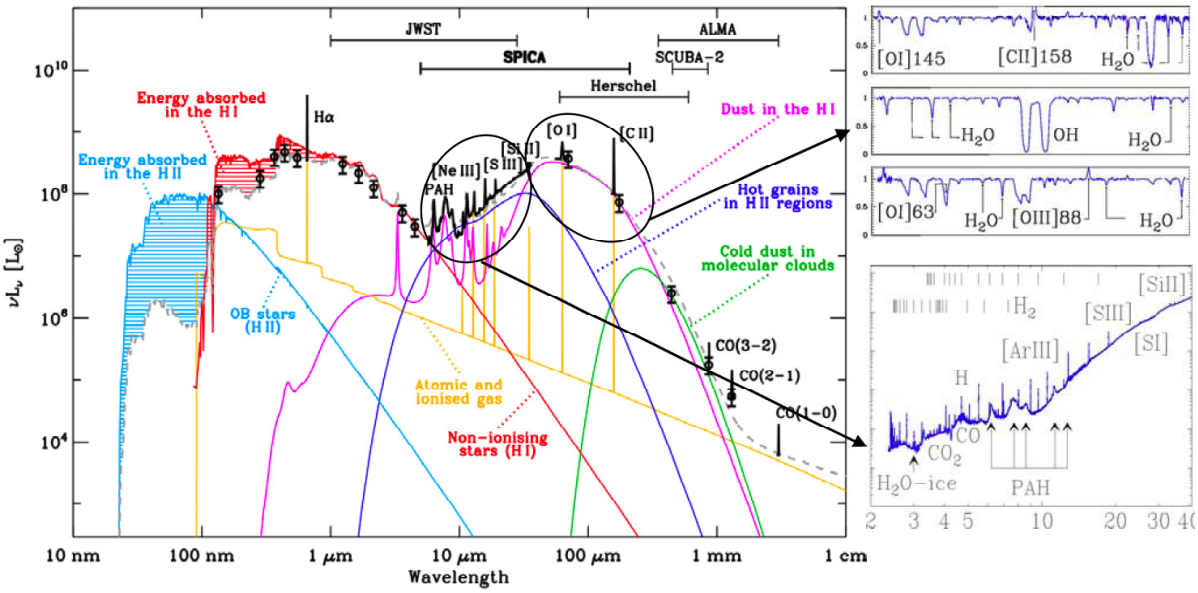

Figure D-2. *Synthetic spectrum of a normal galaxy similar to the Milky Way showing to effect of dust reprocessing of stellar UV/ visible radiation to the mid- and far-IR, and the wealth of spectral features in these bands. Figure from Swinyard et al. (2007) (ISO data on the right from Goicoechea et al. 2004, Polehampton et al. 2007, Rosenthal et al. 2000).*

monolithic telescope and resulting clean point spread function (PSF), it is estimated that a binary mask type coronagraph will achieve a contrast ratio of $<10^{-6}$ at an inner working angle of $5\lambda/D$ (see Enya et al. 2006 for details). This is equivalent to Saturn's orbit at 10 pc for $\lambda=5$ μm. This wavelength targets the younger end of the planet age range, and some ~30 target stars are within 10 pc. It is anticipated that further development should reduce the inner working angle further, increasing the range and target star sample size. The coronagraph includes a spectroscopic capability, potentially revealing biologically-relevant compounds such as methane, water, and ammonia in the planet.

3) Deep unbiased extragalactic mid-IR spectral surveys. SPICA's mid-IR imager / spectrometer (SPICA-MIR) is well-suited to wide-field extragalactic surveys. SPICA-MIR extends the wavelength coverage of JWST / MIRI to 38 μm, and is not impacted by thermal emission from the observatory which degrades MIRI at its longest wavelengths. The SPICA-MIR includes a wide-field low/medium resolution (R~200) objective grism mode with a several-arc-minute field of view allowing blind spectral surveys 10–100 times faster than MIRI. This will be a unique rapid spectral survey capability complementing MIRI's outstanding sensitivity in smaller fields.

4) Deep imaging of distant galaxies at $\lambda<100$ μm. Relative to Herschel, SPICA's cold aperture offers the potential for factors of 10–300 improvement in raw sensitivity, which translates to factors of 10^{2}–10^{5} improvement in mapping speed for a given array size and observation depth. At its longer wavelengths, source confusion will quickly become an important limitation for SPICA, but shortward of 100 μm, SPICA has the angular resolution necessary to directly resolve the bulk of the far-IR background populations. Unlike Herschel at these wavelengths, SPICA ESI has sufficient sensitivity to survey to this depth rapidly over large areas of sky.

5) Sensitive mid-IR to submm spectroscopic surveys will reveal the evolution of processes and interstellar contents in dusty galaxies through cosmic time. These measurements will make use of the ESI and especially the BASS instruments. This is the most exciting prospect for SPICA and requires its full suite of spectroscopic capabilities. These same powerful spectrometers will also be applied to Galactic regions, efficiently probing the Galactic Center and a range of star formation sites.

D.1.3 NASA's Contribution → The BASS Spectrometer

We present here BASS, a far-IR spectrograph for SPICA. BASS is tailored to this SMEX opportunity, and represents a subset of a more

Table D-1. SPICA Instrument Suite

Instrument	Contributor	Description / Capabilities
Mid-IR Imager / Spectrometer	JAXA / KASI	4 channels from 5 to 38 μm. 1k × 1k Si:As and Si:Sb arrays. Imaging and R~200 grism spectroscopy with 100–400 arcsec field of view. Spectroscopy mode: long slit, R=3,000 at 20–30 μm, R=30,000 at 5–15 μm. Tip-tilt mirror shared with coronagraph.
Mid-IR Coronagraph	JAXA / KASI	5–27 μm core range, contrast > 10^6. Inner working angle 2–5 λ/D. Outer working angle, 10–30 λ/D.
ESI	European national agencies	30–200 μm imaging Fourier-transform spectrometer (IFTS), 2′×2′ FOV. R variable from 10 to few × 1000. Detectors TBD Ge photoconductors or bolometers. Ref: Swinyard et al. 2008
BASS	NASA	Grating spectrometer optimized for rapid spectral surveys, Sensitive bolometers at 50 mK. Range: 132–340 μm.

Notes: KASI = Korea Astronomy and Space Science Institute

powerful instrument concept called BLISS (see www.submm.caltech.edu/BLISS) that is beyond the SMEX category as it requires technology development. **Before proceeding, we stress that this window of opportunity for a major U.S. participation in SPICA will only be available for a limited time.** Whether through this proposal or otherwise, study funds are required if NASA is to have a future role in the mission. SPICA is now entering its development phase in early 2008, and technical interfaces will be frozen in the coming year. NASA participation in this phase is necessary to enable the provision of a U.S. instrument.

BASS covers the 132–340 μm wavelength range at a resolving power of 300. The instrument consists of two feedhorn-coupled waveguide grating spectrometers, each with 160 bolometers providing instantaneous coverage over the full band. Both spectrometers observe simultaneously, fed by a chopper mirror which modulates the BASS beams from the astronomical source to a reference position at a period of 2 s to 10 s. The only moving part will be the chopping mirror.

BASS employs semiconducting-sensed bolometers similar to those developed and built at JPL for the Herschel SPIRE and Planck HFI instruments. These silicon-nitride "Spider Web" bolometers have shown excellent performance in a variety of ground-based and suborbital instruments, and the Herschel and Planck arrays have been successfully qualified for flight with performance exceeding design requirements. Because bolometer technology is advancing rapidly, we will conduct trade studies of alternative approaches including superconducting transition-edge-sensed bolometers.

To achieve the necessary sensitivity, the bolometers and waveguide spectrometers in BASS must be cooled to 50 mK. This will be accomplished with a two-stage magnetic refrigerator which provides heat lift at both 50 mK and 400 mK for an intercept stage, and rejects heats to SPICA's 1.7-K cooler. Magnetic refrigerators similar to that proposed for BASS have been built by U.S. groups and flown.

BASS on SPICA will provide a 5-σ 1-hour sensitivity of 2.2–4.4 × 10^{-20} Wm^{-2} in its band. This is 2–4 times better than the goal sensitivity of the ESI, and will extend SPICA's capabilities to redshift 3–4 galaxy populations. There is some wavelength overlap between the two instruments which ensures good calibration. For galaxies accessible to both, the combination BASS-ESI will offers complete spectral coverage across the 30–340 μm range. These capabilities are shown in **FO1, Figure D-A**.

D.1.4 BASS Objectives and Approach

The BASS core science proposed as part of the PI mission will use approximately 1000 hours of SPICA time to chart the history of and mechanisms within LIRG- and ULIRG-class dusty galaxies through what appears to be the era of peak galaxy activity: from redshift 3 to 0.5. There are two approaches:

1) We will measure the powerful far-IR fine-structure transitions of [OI], [OIII], and [CII] to determine redshifts and basic interstellar medium properties in a sample of 500 high-redshift galaxies. The sample will be based on catalogs from continuum surveys, e.g. those of Spitzer, Herschel, Akari, SCUBA2, and SPICA itself, in an attempt to probe the sources that produced the bulk of the stellar mass in the

Far-IR spectroscopy with SPICA: decoding the history of stars, black holes, and heavy elements since Recombination

Cosmic Backgrounds:
The record of all photons ever released in the Universe since Recombination.
Half this energy is in the far-IR

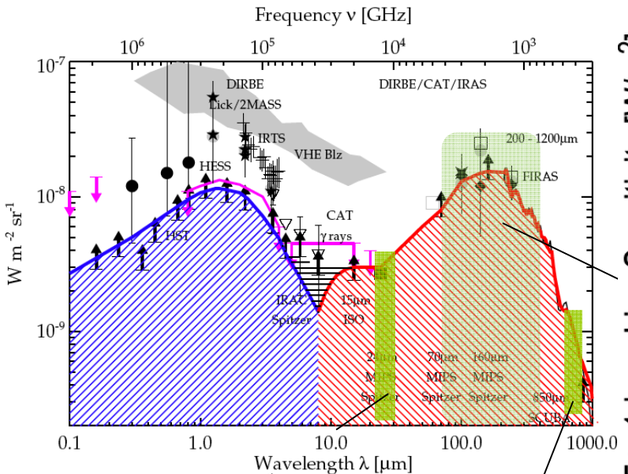

Spitzer MIPS 24 μm

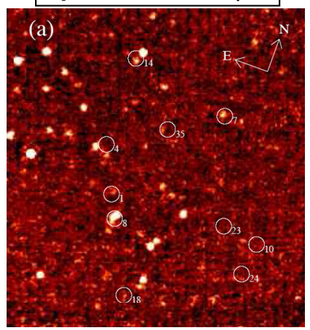

SCUBA / JCMT 850 μm

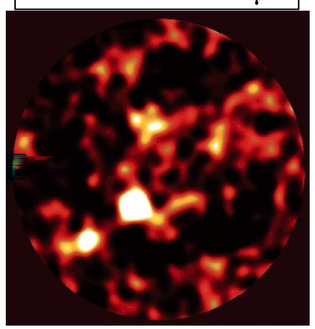

Broad-band imaging is now resolving the bulk of the background: tens of thousands of dusty galaxies, likely at redshift 0.5 to 3.
Even larger cameras on ground-based observatories and Herschel will find tens of thousands more.
Far-IR spectral follow-up is needed to probe the processes hidden behind the dust in these galaxies.

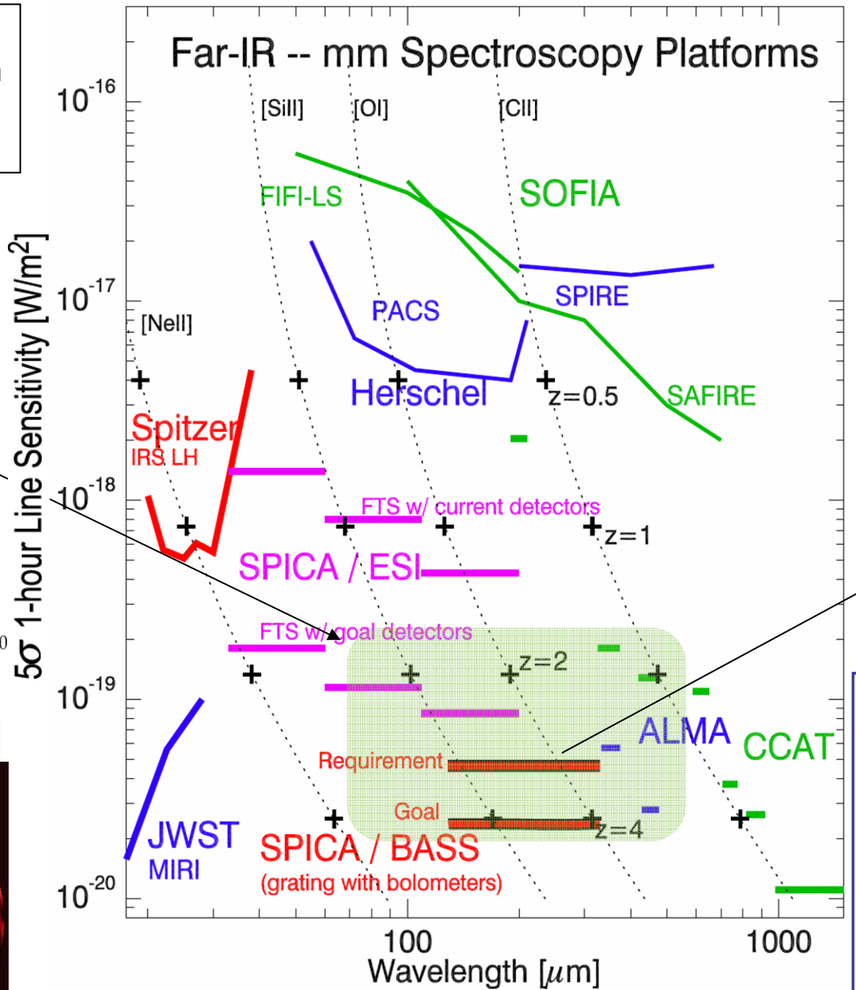

Figure D-A. *Sensitivity of far-IR spectroscopy platforms. Values for SOFIA, Herschel, Spitzer, and ALMA are taken from the instrument web pages. CCAT is a proposed 25-m Cornell-Caltech Atacama Telescope at a high site with background-limited spectrometers in the atmospheric bands. For ALMA, a 300 km/s linewidth is adopted. SPICA ESI sensitivities are taken from the Cosmic Visions proposal / white paper (Swinyard et al, 2008). BASS values include the astrophysical backgrounds and detector NEPs of 2.5 (5) × 10^{-19} W /sqrt(H)z corresponding to the goal (requirement). The Spitzer IRS HiRes curve is the achieved sensitivity of the long-high module. As a guide to the cosmological capability, overplotted are spectral line intensities from ULIRGs at various redshifts assuming a fractional line intensity of 10^{-3} (and Ω_{vac}=0.73, Ω_{mat}=0.27, H_0=71). See also a similar figure which incorporates instantaneous bandwidth to show spectral survey speed on page B-1.*

Far-IR spectra probe all aspects of galaxies

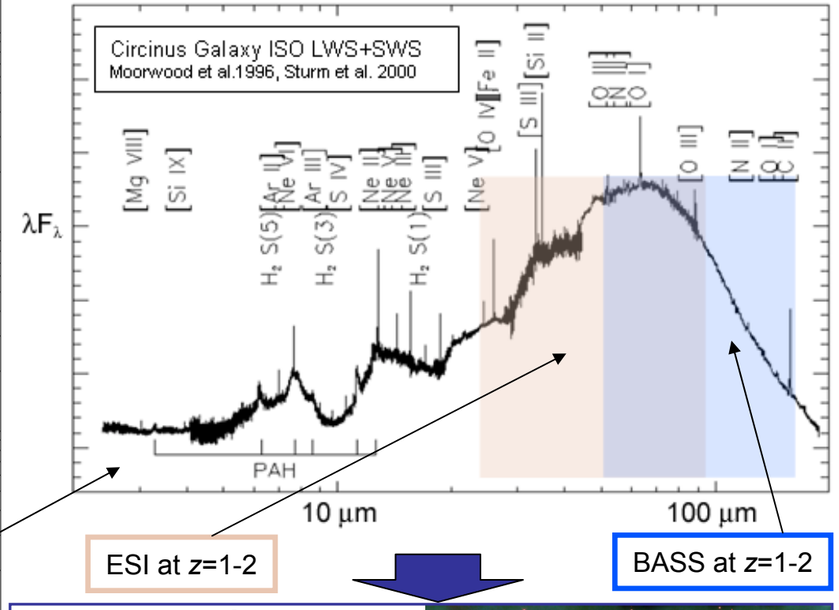

ESI at *z*=1-2

BASS at *z*=1-2

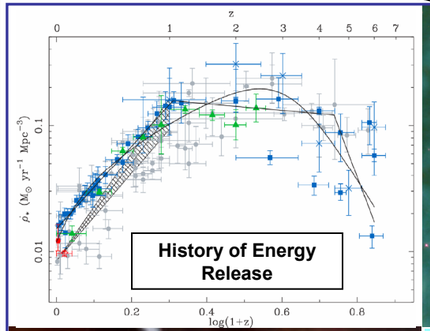

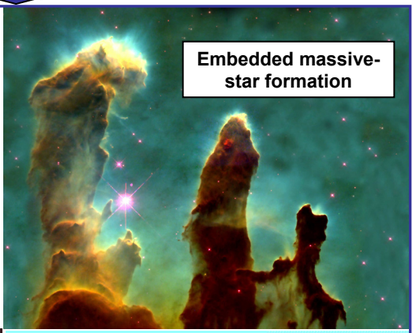

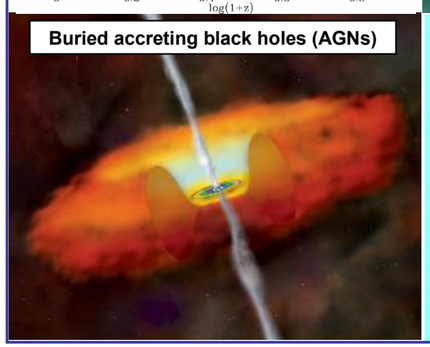

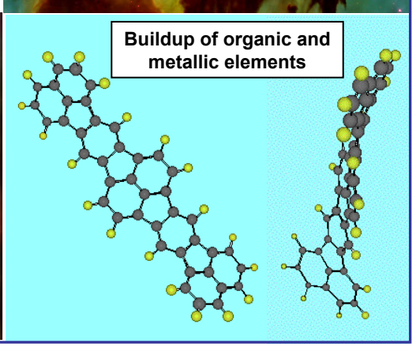

current universe. The [CII] and [OI] lines are the dominant coolants of the neutral ISM gas, and the [OIII] line is an important coolant for HII regions, each can be up to 1% of the galaxy luminosity. The spectral coverage of BASS ensures that at least two of these lines will fall in the band for all redshifts. The frequency ratio immediately identifies the lines and fixes the redshift for each galaxy. The fluxes of the lines in relation to one another and to the far-IR continuum will also reveal basic properties of the power source for each galaxy. The 500 galaxies will provide a statistically significant measure of properties when binned in both cosmic time (log (1+z): e.g.~12 bins) and galaxy power (log L: e.g. ~4 bins). We anticipate that such a survey would require approximately 1 hour per galaxy on average, or 500 hours total.

2) We will then obtain deeper spectra on a sub-sample of 100 galaxies selected from the above parent sample. Each of these more sensitive spectra will require ~4 hours on average, for a total of approximately 400 hours. This sub-sample will be designed to be representative, but also to enable detection of lines with luminosity fractions as low as 10^{-4}, more than an order of magnitude fainter than the dominant coolants. These deeper spectra will reveal the fine-structure transitions of singly- and doubly-ionized nitrogen, as well as the far-IR rotational transitions of molecules: OH, water, and CO, in absorption or emission. These detailed spectra will provide a complete census of all phases of the interstellar gas in these galaxies: ionized, neutral, and warm molecular in the era when the galaxies were most rapidly forming stars. They will also chart the abundances of life-critical elements: C, N, O.

D.2 The Cosmic IR Background (CIB): The Remnant Glow of Dusty Galaxies from their First Formation to the Present Day.

Just as the Cosmic Microwave Background (CMB) is our window into the very early Universe, the optical through far-IR background represents all the energy released since the first stars formed and massive black holes began to grow. This energy, much of which is concentrated in the far-IR (the CIB) provides the record of the emergence of the modern Universe. Spectroscopy with SPICA will penetrate the obscuring dust to reveal how our modern Universe emerged.

D.2.1 Mid- to Far-IR Continuum Surveys

The first step toward understanding the CIB history is to resolve the diffuse background into its individual galaxies through broad-band imaging. Great progress has been made in this direction in the last decade with the first large-format far-IR and submillimeter cameras. Further advances are pending in the next decade with Herschel and even more powerful ground-based cameras. **By the time SPICA will fly, the sources generating the bulk of the CIB will have been discovered, setting the stage for their detailed spectroscopic study with BASS and the other SPICA spectrographs.**

Astronomers have approached the CIB from both sides of the peak, the submillimeter and the mid-infrared. The SCUBA (λ=850 μm) and MAMBO (λ=1.2 mm) instruments were the first large-format bolometer cameras to reveal a population of galaxies that can account for ~60% of the background at these wavelengths (Smail et al. 2002, Chapman et al. 2002, and refs. therein). At shorter wavelengths, MIPS on Spitzer has discovered tens of thousands of galaxies. In the short-wavelength MIPS bands, at 24 and 70 μm, the source counts roll off at the faintest fluxes, indicating that the bulk of the light has been resolved (Chary et al. 2004, Papovich et al. 2004, Frayer et al. 2006). Dole et al. (2006) have taken the important step of using the positions of 24 μm-detected sources to help extract information from the longer-wavelength (70- and 160-μm) datasets. Stacking analysis shows that the 24 mm population appears to add up at 70 μm and 160 μm to account for the bulk of the CIB near its peak wavelength. The conclusion is that the 24-μm populations detected with Spitzer are, at least in aggregate, responsible for most of the cosmic infrared background.

The imaging surveys planned in the coming decade with Herschel and submillimeter ground-based platforms will offer long-wavelength fluxes to better constrain the mid-to-far-IR SEDs of individual objects, but these new imaging surveys alone are unlikely to provide qualitatively new insights into the processes at work in these redshift 1–3 galaxies. The **broadband far-IR continuum surveys provide no information about the galaxies' distances (redshifts), only limited diagnostic power to understand the energy sources within these galaxies.**

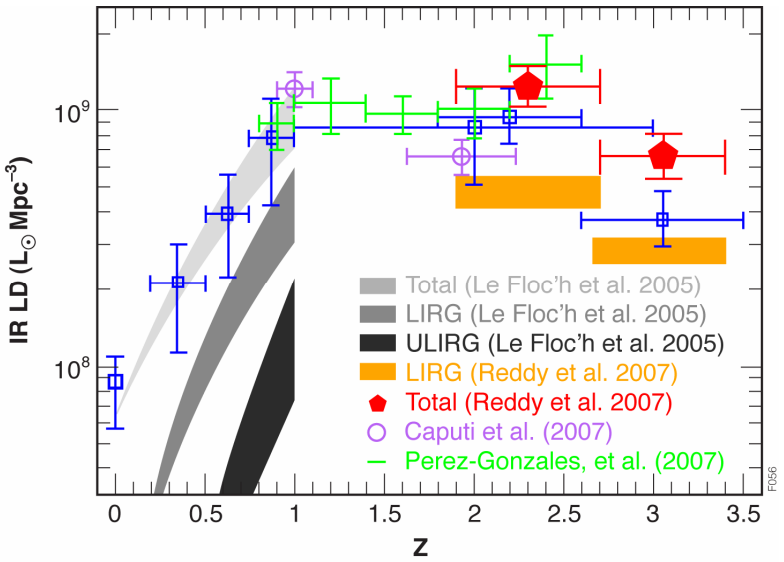

Figure D-3. *The infrared luminosity density as a function of redshift to $z = 3.5$ (taken from Reddy et al. 2007). The blue points represent pre-/non-Spitzer data. The Spitzer-based data include results from Reddy et al. (2007), Caputi et al. (2007), Pérez-González et al. (2005), Le Floc'h et al. (2005). The bands indicate the total, LIRG, and ULIRG contribution to the total infrared luminosity density at $z < 1$, as determined by Le Floc'h et al.*

D.2.2 Far-IR Spectroscopy is a Universal Unbiased Redshift Machine

The first measurements that BASS spectroscopy with SPICA will immediately provide are redshifts. Did the dusty galaxies which produced the CIB undergo the same energy release history as the optically-selected populations? There is mounting evidence that the answer is no. A sample of the submm galaxies, which in principle are suffer very little redshift-selection bias, have redshifts 2–3 measured both with radio/optical follow-up (Chapman et al. 2005), and recently with the Spitzer IRS. (Valiante et al. 2007, Pope et al. 2006). The Spitzer 24 μm-selected sources confirm a dramatic decrease in luminosity from redshift 1 to the present: LeFloc'h et al. infer a shift in characteristic luminosity L* at a rate of $(1+z)^{4.0\pm0.5}$ (**Figure D-3**).

Both the rapid evolution recently, and the potential peak between z=2–3 suggest that the far-IR populations may have had a different history from the optically-selected populations, which appear to have experienced a more constant rate of energy release with cosmic time (e.g. Hopkins et al. 2007). The BASS-SPICA sensitivity of 3×10^{-20} Wm^2 will enable follow-up of the LIRG- and ULIRG-class galaxies at redshifts 0.5–3 which likely produced the CIB in their dominant gas coolants: the powerful [OI], [OIII] and [CII] fine-structure transitions. **Based on the studies of the Spitzer 24-μm and 850-μm populations described above, the BASS-SPICA sensitivities will access the bulk of the CIB populations spectroscopically, including the submillimeter galaxies.**

D.3 Conditions in the ISM in Galaxies at *z*~1–3

At high redshift, the process of star formation and perhaps the conditions around massive black holes are likely to be modified by the lower metallicity of the interstellar medium, as well as potential differences in the structure of typical galaxies. For example, the dust to gas ratio decreases with decreasing metal content (Draine et al. 2007, Engelbracht et al. 2008), and this trend has been invoked to explain differences in the global infrared SEDs of ULIRGs at $z\sim2$ (Rigby et al. 2007). In addition, the morphologies of high-redshift infrared galaxies indicate that many of them are not major mergers (as are most local ULIRGs) but appear to be only modestly disturbed spirals (e.g., Bell et al. 2006, Lotz et al. 2007). These observations suggest that local analogs do not represent well the conditions in the dominant IR galaxy population at high redshift. There are no local low-metallicity ULIRGs and the great majority of local star-forming ULIRGs are dominated by

	Science Objective	Approach	Scientific Measurement Requirements	Instrument/Mission Functional Requirements
BASS Core Science Themes	**Origin of Galaxies in the Universe**	**Measure redshifts and basic processes in galaxies in the early Universe with far-IR spectral surveys for the bright fine-structure transitions**. * [CII] / far-IR assesses physical extent of star formation at z~1. * [OI] / far-IR probes interaction of black holes with host galaxies at z~1-3 * [OIII] line pair measures massive star content at z~2.	On a sample of 500 galaxies, measure bright far-IR lines in LIRG and ULIRG-class galaxies from z=3 to z=0.5 at an average rate of 1 galaxy per hour. **Instantaneous broadband coverage: 130--340 μm.** **Line sensitivity of 5×10^{-20} Wm^{-2} (5 σ, 1 hour).**	Cold SPICA telescope: ~500 hours **BASS** Spectrograph • Resolving power ≥ 300 • NEP ≤ 5e-19 W Hz$^{-1/2}$.
	Origin of Stars and Elements of Life in the Universe When star formation activity peaked, at 1/3 to 1/2 the age of the universe.	**Probe conditions of star formation over cosmic history, through the peak of star formation.** On a sub-sample of high-z galaxies: Extend depth of spectra to include ionized nitrogen and far-IR molecular lines: * Provides a complete census of the ISM: ionized, atomic, and molecular. * Charts carbon, oxygen, nitrogen abundances over time.	With 100 of the above galaxies, obtain complete detailed spectra sensitive to line luminosity fractions as low as 10^{-4} in 3×10^{11} $L_\odot$ galaxies at z=1.5. **Instantaneous broadband coverage: 130--340 μm.** **Line sensitivity 1.5×10^{-20} Wm^{-2} in 4 hours (3 σ).**	Cold SPICA telescope: ~400 hours **BASS** Spectrograph • Resolving power ≥ 300 • NEP ≤ 5e-19 W Hz$^{-1/2}$.
BASS+ESI Open-Time Themes	**Origin of Stars and Planets** In the present era → within galaxies in the local universe	**In the local universe and within the Milky Way Galaxy: probe ISM properties with complete far-IR / submillimeter spectra:** Use fine-structure lines **and** molecular lines to: * Assess stellar mass function through UV-field hardness and intensity. * Distinguish black-hole accretion energy from star formation energy via unambiguous molecular torus signature in high-J CO, H_2O lines.	On a sample of galaxies in the local universe (within 500 Mpc), obtain complete detailed spectra: measure line luminosity fractions as low as 4×10^{-5} in 3×10^{10} $L_\odot$ galaxies within 500 Mpc. **Broadband far-IR coverage -> 40--340 μm** **Line sensitivity of 1×10^{-19} Wm^{-2} (5 σ, 1 hour).**	**BASS + ESI** on SPICA • BASS Resolving power ≥ 300 • BASS NEP ≤ 1e-18 W Hz$^{-1/2}$. (ESI imaging Fourier Transform Spectrometer provided by European consortium—see below)
	Formation of Planets	**Probe the gas disk progenitors of planetary systems via their primary coolants: mid- and far-IR spectral lines**. * Fine structure transitions of Si and O dominate in UV-illuminated regions. * Rotational transitions of water and OH dominate closer to the disk plane.	Survey sources with mid-IR excesses within 300 pc. Expect lines as bright as 1e-19 Wm-2. **Broadband far-IR coverage → 40–340 μm** **Line sensitivity of 1×10^{-19} Wm^{-2} (5 σ, 1 hour).**	**BASS + ESI** on SPICA • Coverage: 40 to 340 μm • Resolving power ≥ 60 • NEP ≤ 1e-18 W Hz$^{-1/2}$.
SPICA O-T Themes	**Direct Studies of Nearby Planetary Systems**	**Goal: detect planets in Saturn-like orbits at 10 pc distance, and obtain their mid-IR spectra revealing pre-biotic materials if present.** Coronagraphy enabled by SPICA's clean PSF, target mid-IR wavelengths where planet / star contrast is greatest.	**Contrast ratio of ≤ 10^{-6}, at angular separation of θ_{min} ≤ 5 λ/D from central star at 5 μm.** **Cover to 27 μm, include spectroscopic capability.**	**SPICA Coronagraph** using hybrid binary shaped-pupil mask and phase-induced amplitude apodisation (PIAA). (see below) Provided by JAXA w/ KASI contribution.
	Evolution of Galaxies via mid-IR Spectral Surveys	**Wide field moderate-spectral-resolution surveys, full zodi-limited mid-IR capability to 38 μm**. Rapid survey capability complements JWSTs exquisite sensitivity in small fields.	**Grism spectroscopy mode in wide-field (100-400 arcsec) mid-IR instrument.** **R~200, λ from 5 to 38 μm**	**SPICA mid-IR instrument** with 1k x 1k BIB arrays, Si:As and Si:Sb. (not shown) Provided by JAXA w/ KASI contribution.

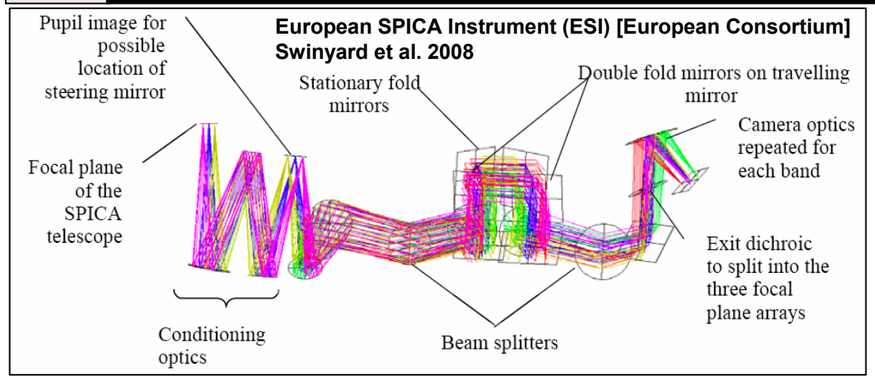

European SPICA Instrument (ESI) [European Consortium]
Swinyard et al. 2008

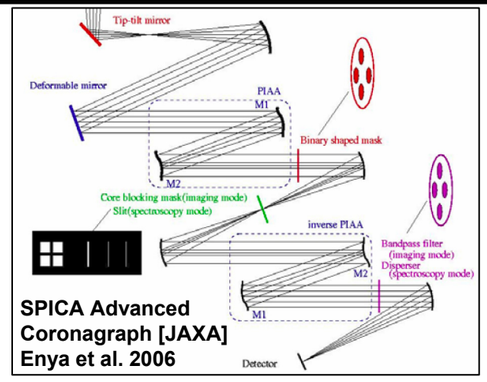

SPICA Advanced Coronagraph [JAXA]
Enya et al. 2006

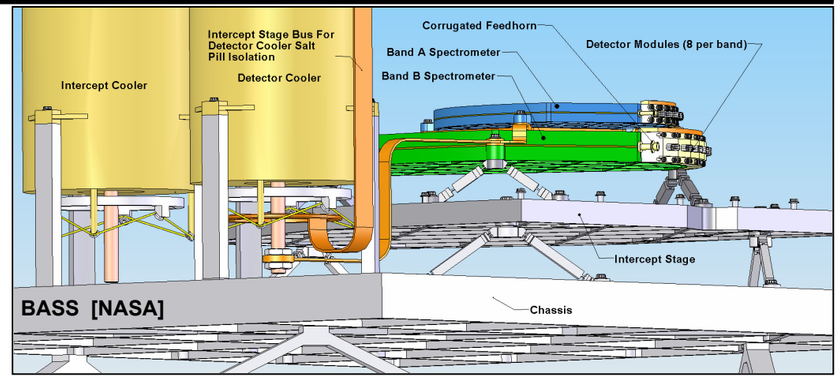

BASS [NASA]

nuclear-concentrated regions of extremely high optical depth in dust.

The conditions in the ISM not only affect the observed properties of galaxies, they also strongly influence the processes that lead to star formation. Optical spectroscopy (probing the rest frame UV) is so strongly affected by extinction that it cannot give a representative view of a high-redshift ISM, while sensitivity limitations make detailed observations in the near-IR (rest optical) impossible. The strong, extinction-free, and highly diagnostic complex of lines accessible in the far-IR are the best observables to support astrophysical analyses of the conditions in the interstellar gas in these galaxies.

D.3.1 A Population of Buried AGN at Redshift 1–3

Papovich et al. (2007), Daddi et al. (2007), and Lutz et al. (2007) have shown through stacking analyses that bright 24-μm sources at $z\sim1.5$ to 2.5 tend to be weaker in the near-IR and at 70 and 160 μm than if scaled from the 24-μm flux with a starburst template. The implication is that these sources have mid-IR excesses due to deeply buried AGNs, and this is confirmed with the stacked X-ray spectrum which shows Compton-thick AGNs. These buried AGNs appear to be numerous, and may account for the growth of black holes required to match the present-day black-hole mass/stellar mass relationship. SPICA will test the interpretation of the Spitzer stacked measurements by probing the properties of the individual sources. BASS in particular will be able to probe the feedback between these AGNs and the interstellar media of their host galaxies.

D.3.2 An Evolving IMF Producing More Massive Stars at Earlier Times

There is growing evidence for a discrepancy between the observed total stellar mass in galaxies, and the stellar mass inferred by integrated the luminosity history to that time and applying standard conversion factors. The observed luminosity history, including both 24-μm and (extinction corrected) UV would produce $\sim$2 times more stellar mass than is observed via rest-frame near-IR photometry at redshift 2.

A recent article by Davé (2007) shows the discrepancy clearly and discusses potential explanations. The most compelling is an evolving stellar IMF which becomes increasingly top-heavy at earlier times. Davé finds that an evolution in the IMF characteristic mass of the form $M^*=0.5\ M_\odot\ (1+z)^2$ is required out to redshift 2, implying that the characteristic stellar mass which is 0.5 $M_\odot$ today is 4.5 $M_\odot$ at redshift 2! Physically, this could be the result of an increased minimum temperature of molecular gas due to increased heating (via increased supernova input or greater UV fields) or decreased cooling (due to lower metallicity). It is intriguing that M82 (Rieke et al. 1980, 1993) and extremely vigorous star forming regions in the Galactic Center (Figer 2005) are seen to be deficient in low-mass stars relative to local IMFs. Do the enhanced star formation rates inferred for higher redshifts also produce top-heavy IMFs? Spectroscopy with BASS-SPICA of the embedded HII regions around new stars in these galaxies will provide constraints on the IMF itself, and on potential physical mechanisms responsible for it.

D.4 The Far-IR Spectroscopic Toolbox

Even for the subset of dusty galaxies for which optical counterparts can be identified and optical spectra obtained, the high obscuration ensures that the optical spectra do not probe the bulk activity in these galaxies. Goldader et al. (2002) and others have demonstrated this, showing that luminosities based on UV/blue fluxes and colors underestimate the total luminosities of a sample of LIRGs and ULIRGS by factors of 3–75, and that the UV/optical light often comes from regions hundreds of parsecs from the true luminosity sources. **Far-IR–submillimeter spectroscopy is the natural probe of astrophysics in dusty galaxies because it is immune to dust extinction, and therefore probes the entire galaxy**. Unlike the mm-wave tracers available from the ground at longer wavelengths, the far-IR–submm transitions access all important components of interstellar gas–molecular, neutral atomic, and ionized (**Table D-2**). We will study in detail a subsample of 100 of the $z\sim1$–3 galaxies in our core program to reveal the complete suite of far-IR lines. In this section we outline the wealth of astrophysical information available with the lines traced with BASS, and in some cases the other SPICA spectrographs.

D.4.1 The Impact of New Stars on their Birthplace: HII Regions and Photo-Dissociation Regions (PDRs)

The UV radiation from newly-formed high-mass stars within molecular clouds strongly affects

Table D-2. Spectral Features Available to SPICA

Species	Wavelength [μm]	I.P. [eV]	f_{M82}	f_{A220}	Diagnostic Utility
			Ionized Gas Fine Structure Lines		
Ne V	14.3, 24.3	97.1			Primarily AGN
O IV	25.9	54.9			Primarily AGN
S IV	10.5	34.8	2.1×10^{-5}		Probes gas density and UV field hardness in
Ne II	12.3	21.6	1.2×10^{-3}	7.5×10^{-5}	star formation HII regions.
Ne III	15.6, 36.0	41.0	2.05×10^{-4}		"
S III	18.7, 33.5	23.3	1.0×10^{-3}	7.3×10^{-5}	"
Ar III	21.83	27.6	9.1×10^{-6}		"
O III	51.8, 88.4	35.1	1.3×10^{-3}		"
N III	57.3	29.6	4.2×10^{-4}		Diffuse HII regions
N II	122, 205	14.5	2.1×10^{-4}		
			Neutral Gas Fine Structure Lines		
Si II	34.8	8.2	1.1×10^{-3}	7.7×10^{-5}	Density and temperature probes of
O I	63.1, 145		2.2×10^{-3}	-6.8×10^{-5}	photodissociated–neutral gas interface
C II	158	11.3	1.6×10^{-3}	1.3×10^{-4}	between HII regions and molecular
C I	370		6.2×10^{-6}	1.2×10^{-5}	clouds and around AGN
			Molecular Lines		
H_2	9.66 12.3, 17.0, 28.2		2×10^{-5}	3×10^{-5}	Mass of warm (few 100K) molecular gas
HD	37, 56, 112				D/H ratio
LiH	112, 135, 169, 225, 338				Li/H ratio
CH	149			-4×10^{-5}	Ground state absorption, gives column and
OH	34.6, 53.3, 79.1, 119		-2×10^{-6}	-2×10^{-4}	abundance.
OH	98.7, 163			5×10^{-5}	Emission → temperature & density
H_2O	73.5, 90, 101, 107, 180			$\pm 5 \times 10^{-5}$	
CO	~2600/J = 130, ..., 217,				High-J, T > 200 K molecular gas, e.g. torus
CO	237, ..., 260, ..., 325, 372		3×10^{-6}	(1×10^{-5})	Mid-J, 50 K < T < 200 K mol. gas
			Dust Features		
Silicate	9.7, 18				Dust tracer, also seen in QSO emission
PAH	6.7, 7.7, 8.5, 11.3,				Small transiently-heated grains

Note: The f_{M82} and f_{Arp220} are the ratios of the line luminosity to the total bolometric luminosity.
Shaded lines indicate the key spectral features available to BASS at redshifts 0.5–3.

the natal molecular ISM. Within the immediate vicinity hydrogen is fully ionized forming an HII region whose size is set by cloud density and the number of H ionizing (Lyman continuum) photons that are available. Just beyond the HII region far-UV (6 eV < hν < 13.6 eV) photons penetrate the neutral gas where they photo-ionize atoms and photo-dissociate molecules with ionization or dissociation potentials less than 13.6 eV forming photodissociation regions (PDRs). The depth of the PDR is determined by the extinction of far-UV photons by dust. Halfway through the PDR column, the far-UV field strength **G** (parameterized in units of the local far-UV radiation field, Go=1.6 x 10^{-3} erg/s/cm^2) is reduced to the extent that H_2 becomes self-shielding, and from this point further into the cloud, hydrogen is in molecular form. The heating of the gas in PDRs is primarily through the photo-electric ejection of energetic electrons from grains, with typical efficiency ~1%. Most of the remaining stellar energy goes into heating the grains, which re-emit the energy in the far-IR continuum (e.g. Tielens & Hollenbach 1985). PDRs are an important ISM component—typically 10% by mass in normal Milky-Way-like galaxies, and up to 50% in starburst nuclei and low-metallicity dwarfs.

The primary coolants of these dense PDRs, as well as moderate density "atomic clouds" are the [CII] 158 μm and [OI] 63 μm fine-structure lines. These lines are often the brightest single lines from star forming galaxies, each line can carry up to 1% of the total far-IR luminosity. Observing both lines together with the far-IR continuum constrains the physical conditions of the gas (temperature, density, mass), the area

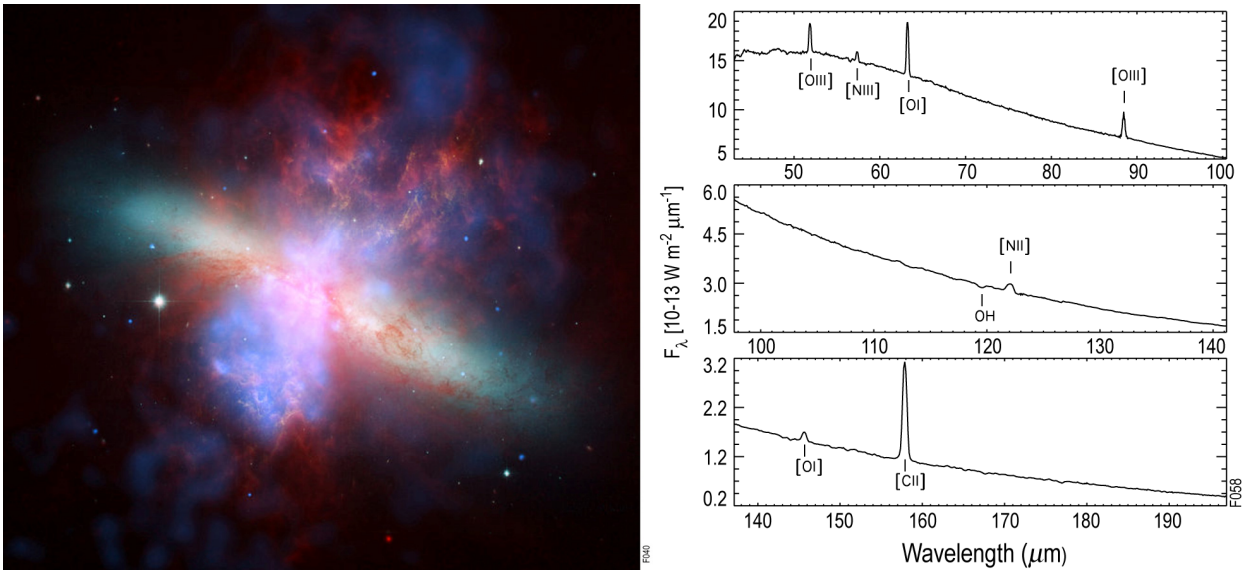

Figure D-4. *LEFT: The nearby starburst galaxy Messier 82, shown in a composite of images from the Chandra X-Ray telescope (blue), Hubble Space Telescope (Hα — orange) and Spitzer infrared telescope (8-μm PAH – red), with colors adjusted to fit everything into the visual spectrum. (Credit: NASA/JPL-Caltech/STScI/CXC/UofA/ESA/ AURA/JHU). RIGHT: Spectrum of the nucleus of this galaxy in the far-IR where it emits most of its energy obtained with the ISO LWS (Colbert et al. 1999). The fine-structure transitions in this spectrum are the primary coolants of the interstellar gas, and are among the most powerful spectral lines emitted by the galaxy. The suite of lines probes the conditions of the starburst, including the masses of the most massive stars. BASS on SPICA will measure these lines in galaxies at redshifts of 1–3, the historic peak of star formation activity.*

filling factor of the emitting gas region and the strength of the far-UV radiation field.

The ionized gas close to the stars can be probed with line pairs (e.g. those of [NII], [SIII], [OIII]) which are density tracers. The intensity ratio of the two lines of a given ion provide a direct density measurement, enabling a distinction between low density HII regions associated with aging stellar populations, and the dense HII regions characteristic of young starbursts. Lines from different ionization states within an element (e.g. [OIII] & [OIV]; [NII] & [NIII]; [NeII], [NeIII], & [NeV]) yield the hardness of the stellar radiation fields, hence identifying the masses of associated main-sequence stars. This is a measure of the age of the starburst, or its initial mass function. In addition, lines from different elements within a given ionization zone (e.g. [OIII] and [NIII]) yield relative elemental abundances, hence the history of stellar processing (e.g. Lester et al. 1987).

An excellent example of the utility of the far-IR lines is the Colbert et al. (1999) study of M82 using seven fine structure lines detected with the ISO LWS (**Figure D-4**). In their analysis the line fluxes were used to probe the star-forming ISM and constrain the stellar populations in M82. The best fit is a 3–5 Myr burst with a 100 $M_\odot$ cutoff, and the line intensities require that half the total mass in the central few hundred pc is involved in the starburst. **The BASS wavelength range is comparable to the ISO LWS range redshifted to $z\sim1$–1.5, and BASS-SPICA will have the sensitivity to make these kind of measurements on LIRG-class galaxies at this distance.**

D.4.2 [CII] Surveys Chart the Evolution of Galaxy-Wide Starbursts

The full suite of far-IR lines is clearly very powerful, **however we point out that measurement of the [CII] intensities alone will provide important insights into star formation at high redshift**—both the strength and spatial extent of the starburst. The [CII]/far-IR continuum luminosity ratio, R, is strongly inversely proportional to UV field strength G for G $\sim10^1$ to 10^4, maximizing at $\sim$1% for G$\sim$10 and n$\sim10^3$ cm^{-3} (**Figure D-5**). The inverse relation occurs because the efficiency of photoelectric heating is reduced at high **G** due to the build-up of grain

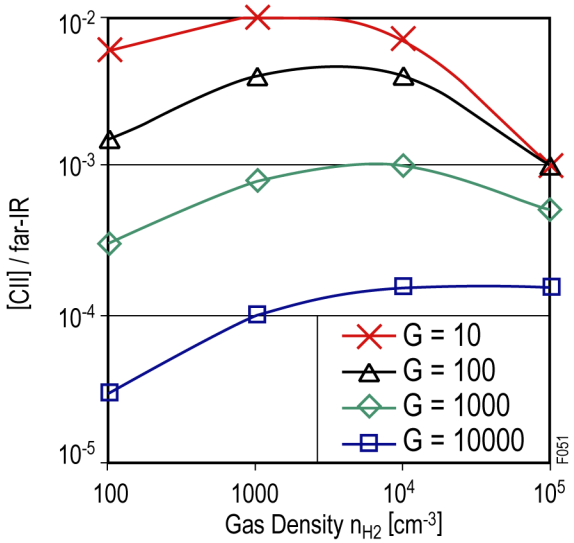

Figure D-5. *Ratio of [CII] to far-IR continuum as a function of PDR density for various values of UV field strength G (from Kaufman et al. 1999).*

charge, and because of the increased gas cooling via the [OI] 63 μm line. Therefore, within these ranges for **G** and **n**, the measurement of **R** determines **G**. In PDRs, dust absorbs most of the far-UV photons, and re-radiates the energy as far-IR continuum. Thus on small scales where the emitting region is resolved, the far-IR intensity should equal the inferred UV intensity **G**. Galaxies are not resolved, so the ratio of the observed far-IR continuum flux to inferred **G** is the beam filling factor, or for unresolved galaxies the physical size of the starburst region in kpc^2.

Recently, the [CII] line was detected from FSC 10026+4949, a hyperluminous galaxy at z=1.12 (Hailey-Dunsheath et al. 2008). The line is remarkably bright, R~10^{-3}, hence G~1000 (assuming n~$10^3 \rightarrow 10^4$ cm^{-3}, **Figure D-5**). The inferred size of the starburst is >4 kpc in radius, so that this galaxy is undergoing a global starburst. These results are consistent with the large (10-kpc scale) extent of the starburst inferred for 8/12 submillimeter galaxies based on imaging in the radio continuum and rest-frame UV (Chapman et al. 2004). Chapman et al. conclude that star formation in most SMGs is both vigorous (~45 $M_\odot$/yr/kpc^2) and extended with sizes ~45 kpc^2.

The Hailey-Dunsheath [CII] result and the Chapman et al. imaging suggest that most powerful high-redshift sources are unlike the typical local ULIRG, for which the starburst is spatially confined, and the [CII]/far-IR is typically weak (Luhman et al. 1999). Is this difference a luminosity selection effect? Possible, as the SMGs and high-z C+ sources studied to date are extreme objects with L~10^{13} $L_\odot$. Or is the mode of star formation in LIRG+ galaxies fundamentally different when the Universe was half its current age? **With BASS on SPICA we will answer this question with surveys of [CII] intensity in galaxies as weak as 10^{11} $L_\odot$ from z=1.1 to the present day.**

D.4.3 [OIII] Reveals Massive Stars

Due to its relatively high formation potential (35 eV), only very early type (O7 or earlier) stars form HII regions with strong [OIII] line emission. For such HII regions, at a given density, the strength of the 88 μm [OIII] line is proportional to the number of photons capable of forming O++, Q(O++). By detecting both the 52 and 88 μm lines of [OIII], one can determine the ionized gas density, so that the two lines together yield Q(O++). The ratio of Q(O++) to the total far-IR continuum, which traces the total stellar population, thus constrains the relative fraction of massive stars in the source. **With BASS we will measure this [OIII] line pair in galaxies from redshift 1.5–2.7, making an unequivocal test of the top-heavy IMF scenario described above.**

D.4.4 The Impact of Black-Hole Accretion on the Host Galaxy: X-ray Dominated Regions (XDRs)

The second principal source of energy in galaxies is accretion onto black holes. For interstellar material within ~1kpc of a nuclear accretion source, the X-rays are likely to be the dominant heating source. In this case, the energy impinges on the ISM in the form of X-rays, not UV photons creating an X-ray dominated region (XDR). X-rays are not susceptible to dust extinction and propagate directly through the bulk of the ISM, heating the gas directly. The result is that for XDRs, the gas receives a large fraction of the total X-ray input energy, unlike in PDRs (Maloney 1999; Meijerink & Spaans 2005; Maloney, Hollenbach, & Tielens 1996). The large penetration depth of the XDR translates to approximately uniform conditions over large regions, in contrast with the PDR for which the conditions vary quickly as the UV is attenuated upon entering the cloud. XDRs can exhibit a range of physical and chemical conditions, depending on the gas density and the X-ray flux. In general, XDR gas is cooled by the

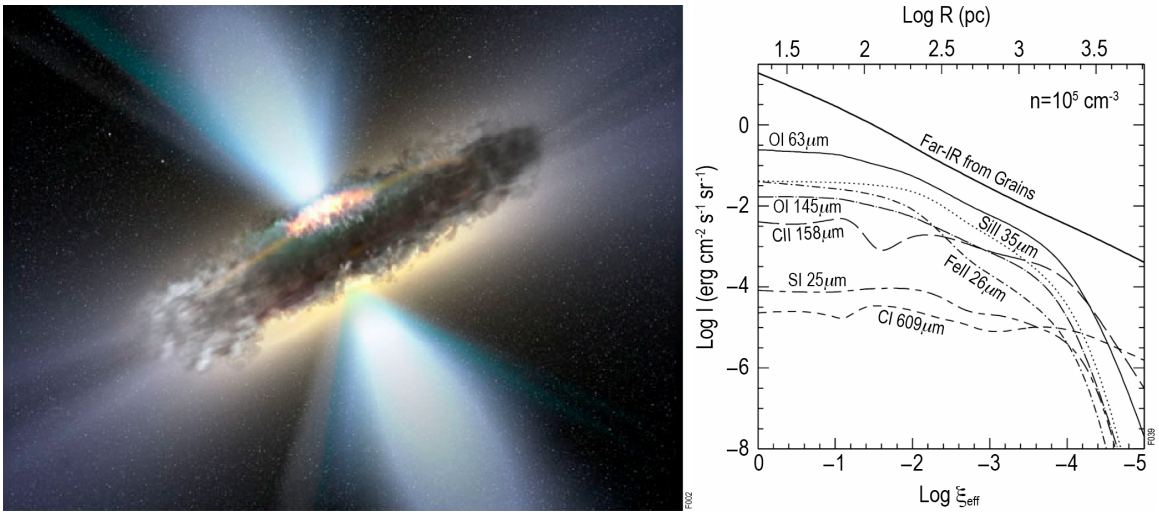

Figure D-6. *LEFT: Artist's concept sketch of an AGN with confining molecular torus (credit: ESA). RIGHT: Cooling of an X-ray Dominated Region (XDR) from Maloney (1999). In an XDR, the widely-distributed gas can receive a large fraction of the total heat input and the fine-structure lines can carry a much greater fraction of the total cooling than in a PDR. As with a star-formation PDR, ratios of line intensities to one another and to the total IR constrain the XDR properties: gas density, input X-ray flux.*

same atomic and molecular lines as in the PDR, with some contribution from gas-grain collisions at high densities. **However, because the XDR gas is directly heated with the X-rays, it is possible that individual lines in particular [OI] can re-emit as much as 10% of the total XDR input energy, much more than the typical 0.3% output in these transitions in PDRs.** This will lead to much larger fractional line luminosities than in typical PDRs. **Figure D-6** illustrates this with a calculation from Maloney et al. (1999).

The recently-discovered population of $z\sim1$–3 Compton-thick AGNs described above (Daddi et al. 2007) should be detectable in [OI] with BASS-SPICA. In nearby galactic nuclei, Dale et al. (2004) have used ISO LWS data to show that Seyfert galaxies show enhanced [OI] emission relative to their starburst counterparts. But the Daddi et al. population is in the peak of AGN activity and represents much more powerful sources: they estimate a mid-IR luminosity in these buried AGNs on order $\sim3\times10^{11}$ $L_\odot$, 5 times more powerful than the local analogue NGC 1068. These AGNs will certainly deposit energy into the gas, and if the XDR models of Maloney et al. and Meijerink and Spaans are correct, the 63 μm [OI] line should have a large fraction of the mid-IR dust luminosity of the AGNs. A line with even 3% of the typical 3×10^{11} $L_\odot$ mid-IR excess would be easily detected with BASS-SPICA at $z=2$. The far-IR and [OI] provide a powerful probe of the dust and gas around the AGN and allow a quantitative measure of the impact of the black hole on the ISM around it. This may provide our most sensitive search for buried AGN in IR-luminous dusty galaxies at these epochs.

D.4.5 Dense Molecular Gas: Rotational Transitions of Hydrides and High-Excitation CO

In the Milky Way and nearby galaxies, UV-shielded molecular gas accounts for about half of the interstellar medium by mass. Since it is the birthplace of stars, understanding the heating and cooling of molecular gas constrains theories of star formation. For typical molecular material, CO is regarded as the most important coolant, and $J=1\rightarrow0$, $J=2\rightarrow1$, and $J=3\rightarrow2$ transitions have been the standard measure of molecular gas mass due to their accessibility. However, observations up to $J=7\rightarrow6$ the highest-frequency transition accessible from the ground now show that much of the molecular gas in starburst galaxies is heated to 100 K or more by stellar UV, turbulence, or cosmic rays. (Bradford et al. 2003, Weiss et al. 2007). This implies that the $J \leq 7$ lines alone are insufficient probes of the temperature, energetics, or mass of the molecular gas in these cases. The mid-J (J=8—15) far-IR CO transitions accessible to BASS at low to moderate redshift are a critical

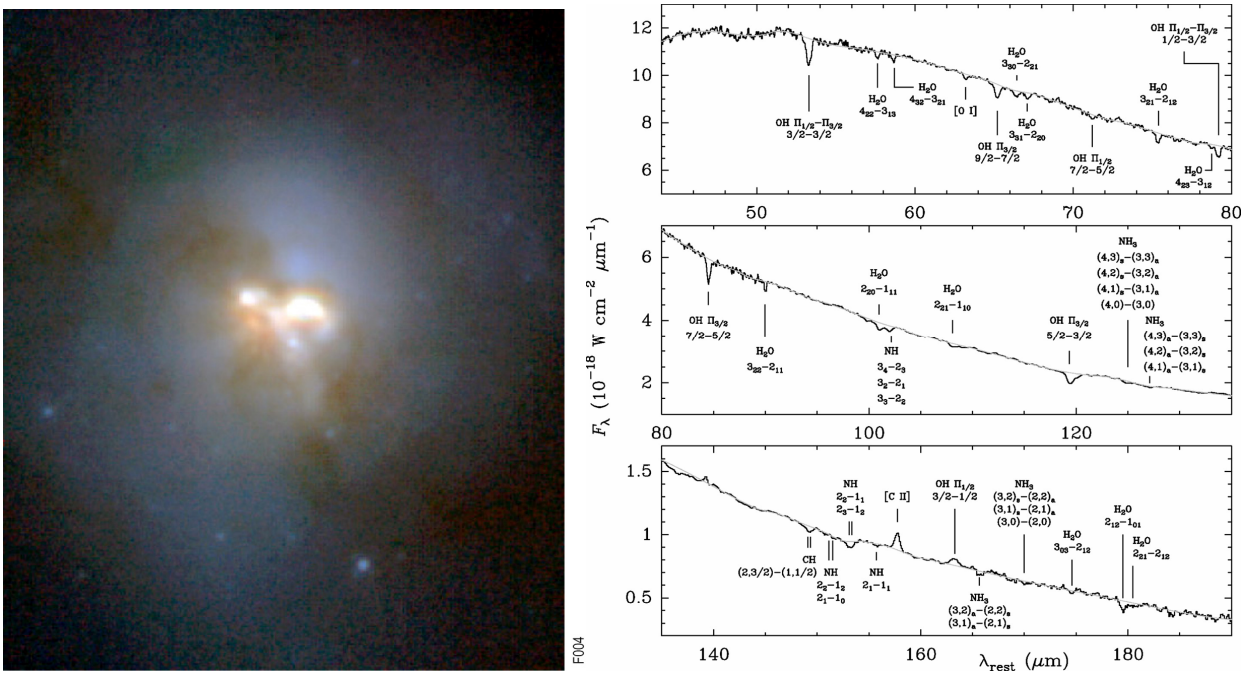

Figure D-7. *The ultraluminous infrared galaxy Arp 220. LEFT: Optical image of the galaxy, showing a fraction of the star formation stimulated by the recent merger of two spiral galaxies (credit NASA). RIGHT: Spectrum of the galaxy in the far-IR, where most of the power emerges. The spectrum was obtained with the ISO Long Wavelength Spectrometer (LWS) at a resolving power of 200, and shows a host of absorption lines tracing the massive molecular reservoir which powers the star formation (Gonzalez-Alfonso et al. 2004). In this highly-obscured source, the OH absorption lines are among the most powerful spectral features.*

complement to the ground-based observations to reveal the full molecular gas energy budget.

For even more extreme molecular material such as that associated with protostellar condensations, shock-excited gas, and AGN tori, the dominant coolants are the light hydrides: OH, CH, and H_2O, and high-J CO. The hydrides have rotational fundamentals in the far-IR, and rapid radiative rates. In the dustiest of galaxies in the local universe, these lines are often seen in absorption, providing a direct measure of column densities and abundances of optically thin species. An example of this is shown in the far-IR spectrum of Arp 220 from Gonzalez-Alfonso et al. (2004), reprinted in **Figure D-7**.

In particular for the torus around an AGN, the high-J CO lines are expected to be very important coolants due to the high density (10^7 cm^{-3}) and temperature (~1000 K). Krolik and Lepp (1989) estimate that in these extreme regions, a single CO line (e.g. J=40->39) at 70 μm can have up to 1% of the input X-ray flux, making it detectable with BASS-SPICA at redshift 1 for a luminous AGN such as those described above. Unlike the more powerful, but more ubiquitous [OI] transition the high-J CO is a "smoking gun." These levels are not appreciably excited in even the most extreme starburst—they unambiguously signal a molecular torus obscuring an accreting black hole.

With BASS, we will measure these crucial far-IR molecular tracers in galaxies at redshifts of 1–2, when conversion of molecular mass to stars and black holes was greatest.

D.5 Observing Strategy, Confusion Considerations

Source confusion has been a major limitation in traditional direct broadband imaging and high-redshift source extraction at the long far-IR wavelengths. However, simple arguments show that the spectroscopic observations we will undertake will not be limited in the same way. The key difference is that unlike a continuum flux, the spectral information produces a meaningful signal when differenced from a nearby reference position. Our survey does not require sources to be extracted based on their brightness relative

to the aggregate background, but instead to follow up known sources with positions determined by other means.

The sources will be based on shorter-wavelengths images. In practical terms the space density of BASS sources will be similar to the space density of sources in the surveys which are resolving the bulk of the galaxy populations. A prime example is the Spitzer 24- μm populations. The source density is on order 15 per square arcminute (Chary et al. 2004, Papovich et al. 2004). This means that there will be on average 0.5 sources per 200-μm BASS-SPICA beam. This density is too high for this source to produce a signal in a continuum map, because the broadband flux in the target beam is nearly indistinguishable from the flux in adjacent beams. However, because the spectral lines will vary from beam to beam, a source density of order unity will be adequate to ensure that the spectral information gathered belongs with the intended 24-μm source. A sanity check is the cover page image, which shows a Hubble Deep Field image with appropriately-sized BASS Band-A beams overlaid. Even in this very deep optical image, it is clear that with careful sample selection, it will be possible to follow-up galaxies unambiguously. An important thrust of our Phase-A study will be to apply the far-IR / submm population models of co-I Scott Chapman to the BASS-SPICA beamsize, sensitivity, and chop-difference observing mode to quantitatively assess these issues.

D.6 Gas in Protoplanetary Disks

Most young stars are surrounded by accretion disks which are likely the progenitors of planetary systems. The disk is transformed in the course of a few 10^7 years to be largely devoid of gas (Zuckerman et al. 1995, Pascucci et al. 2006), and optically thin in dust. At this point, the planet-formation process must be well underway. The evolution of the dust during this period is well constrained by observations, but there is little observational insight into the evolution of the gas.

Measuring the evolution of the gas content of disks from the protoplanetary to transitional stages ($<10^5$ years to 10^7 years) will let us witness the rate of gas dispersal from disks and the conditions within the gas. These measurements will expand our understanding of the conditions for the formation of giant planets as well as the embryos that are the seeds for terrestrial planets. For example, they can potentially discriminate between two competing theories of giant-planet formation. In the traditional scenario, giant planets form via accretion of gas onto rocky cores of a few earth masses (e.g. Kornet et al. 2002 and refs therein). In an alternative picture, they form via gravitational instabilities in the gas disk: gas clumps contract to produce the planets (e.g. Boss 2003). The first scenario requires the bulk of the gas to last longer than the optically-thick dust, while the second is consistent with a more rapid gas dissipation.

In the terrestrial planet region of the disk, the residual gas content of the disk at the epoch when embryos or protoplanets assemble to form terrestrial planets helps determine the ultimate mass and eccentricity of the planet and therefore its eventual habitability. (Agnor & Ward 2002, Kominami & Ida 2002, 2004). In particular, a finite range of gas masses produces earth-mass planets on circular orbits. If the gas mass inside 3 AU at ages of $10^{6.5}$–10^7 yr is much greater than 10^{-2} M_J, the tidal interaction of the planets with the gas is sufficient to circularize the orbits of lunar-mass protoplanets, making it difficult for collisions between them to build earth-mass planets. On the other hand, if the gas inside 3 AU is much less than 10^{-2} M_J, earth-mass planets can be produced but in orbits considerably more eccentric than that of the Earth.

Spectral lines in the mid-IR to submillimeter are among the primary coolants of gas disks, and thus the best probes of their masses and conditions. BASS co-I Uma Gorti has modeled gas disks, and finds that water, CO, and [OI] are the dominant coolants for primordial and debris disks (see **Figure D-8** and Gorti & Hollenbach 2004, 2008). These species are also important chemically, and water in particular bears on the question of habitability. Watson et al. (2007) have recently discovered mid-IR water emission in only one of 30 Class-0 systems surveyed with the Spitzer IRS. Does this reflect a short-lived phase with warm, dense planet-forming gas, or is the Spitzer result simply an orientation effect? The longer-wavelength transitions of water and the other species accessible to SPICA will provide the answer; they carry the bulk of the total water luminosity, as gas temperatures are typically 100–300 K and they are not subject to optical-depth effects. The sensitivity of the cold telescope is crucial; while Herschel and SOFIA will be sensitive to the handful of systems within

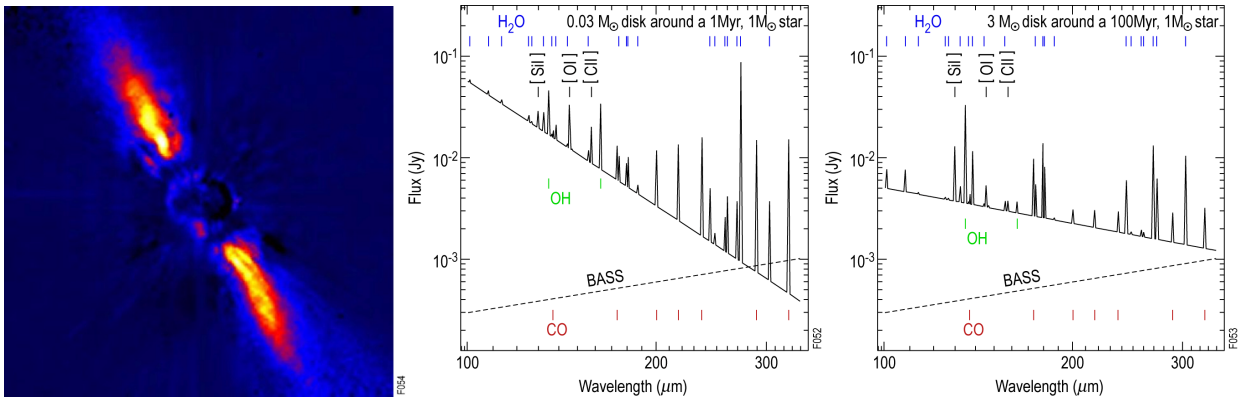

Figure D-8. *SPICA Diagnostics of gas in planet-forming disks. LEFT: Image of Beta Pictoris, a nearby (d=20 pc) disk system. (credit ESO/VLT, J.L. Beuzit et al.) CENTER: Spectrum of a 0.03 $M_\odot$ disk around a Myr-old solar-mass star at 150 pc characteristic of a young system. RIGHT: The same system, but as it might be seen evolved after 100 Myr, after which most of the gas is likely depleted. Intensities are appropriate for the BASS resolving power (R=300), showing that BASS can probe all stages in gas disk evolution. Models after Gorti and Hollenbach (2004, 2008).*

~50 pc (for which there are only a few young systems), **BASS and ESI will enable a statistically significant survey out to hundreds of parsecs, addressing the fundamental problem of gas evolution in these disks.**

D.7 Sensitivities of Far-IR Platforms

The far-IR is one of the few remaining frontiers in the electromagnetic spectrum, where huge improvements in observing speed are still achievable due to the rapid and continuing progress in detector sensitivity, array format, and mission architecture. The critical combination is a modest cryogenic aperture with a sensitive spectrometer.

Substantial gains are still possible in the far-IR because existing far-IR spectroscopy platforms operate far from the ultimate sensitivity limitation: photon noise from the diffuse astrophysical background. The background is produced by interplanetary and interstellar dust, the cosmic far-IR background and the CMB. Careful analysis of COBE DIRBE data (Arendt et al. 1998, Kelsall et al. 1998) has revealed the components, and it is straightforward to calculate the resulting sensitivities. In regions of low zodiacal light and cirrus, the photon noise on a cold telescope can be four orders of magnitude lower than that produced by a passively cooled (~80 K) telescope such as Herschel. This translates into factors of 10^7–10^8 speed improvement in obtaining a complete spectrum for a distant galaxy. The BASS instrument proposed here for the SMEX MoO is not quite at the background limit, due to the use of semi-conducting bolometers described in Section E.5, but will still be a huge step forward, as shown in **FO1** and page B-1.

D.8 BASS Instrument

We now present the key technical elements which make BASS unique: the optical, detector, and sub-K cooling systems. Section E contains further details on our systems approach and the more traditional aspects of the instrument.

D.8.1 Instrument Philosophy, Architecture

The architecture philosophy is based on the aims of the scientific investigation outlined in Section D.2–D.6: broadband follow-up spectroscopy of unresolved sources with known positions. The instrument therefore aims to provide maximum sensitivity at moderate resolving power with complete instantaneous spectral coverage. Spatial multiplexing (imaging/mapping) is a secondary goal. Heterodyne spectrometers are not well-suited to cold space telescopes because they suffer from quantum noise—a term that is factors of 100–1000 times greater than the photon noise from the natural backgrounds. Moreover, the heterodyne backend bandwidths are insufficient for effective spectral surveying.

Direct-detection spectrometers are the natural choice, and the broad bandwidth requirement permits two basic options: diffraction gratings and Fourier-transform spectrometers (FTS). With suitable detectors, the grating

Table D-3. Overview of Technology Heritage

Hardware	TRL	Heritage	Adaptations
NTD Ge bolometers	6–8	Herschel, Planck, Z-Spec, Boomerang	Change NTD doping Reduce G 1-D arrays
JFET readouts	8	Herschel	None
Warm electronics	8	Herschel	None
WaFIRs spectrometer	6	Z-Spec	Reduce dimensions for shorter λ, fixed R
ADR	9	XRS, sounding rockets	Add 400 mK intercept
Chopper	9	Herschel/HIFI, Spitzer/MIPS	Small amplitude

Table D-4. Control of Systems Issues

Hardware	TRL	Heritage	Adaptations
Straylight suppression	6	Z-Spec	Add 1.7 K shield
EMI/EMC suppression	8	SPIRE/Herschel, HFI/Planck	None, but must test to SPICA environment
Microphonic noise suppression	8	HFI/Planck	None, but must test to SPICA environment
Temperature stabilization	8	HFI/Planck	Reduce as BASS requirements are less demanding

spectrometer is more sensitive for observations of a single point source. BASS is therefore a broadband grating, optimized for the very best sensitivity for a given detector choice.

To stay within the SMEX budget and schedule constraints, we selected an instrument based on proven technologies (see **Table D-3** and **D-4**), and chose a limited spectral band with the most promising science given the detector formats available. BASS uses 320 detectors in two WaFIRS spectrometers (described below). Each spectrometer is a duplicate of the Z-Spec spectrometer, simply reduced to accommodate shorter wavelengths. A single spectrometer covers a factor of 1.6 in wavelength, thus the two-band system provides a factor of 2.56 in coverage. We do point out that much of our cost is non-recurring engineering and hardware (e.g. the refrigerator) so the marginal cost to add more bands would be modest, and would not substantially impact our interfaces.

The BASS range was chosen to provide coverage shortward of the 350-μm window accessible from the ground: the chosen range is 130 to 340 μm. in two bands (see **Table D-5).** This choice complements the proposed ESI spectrometer by extending the capability to beyond 200 μm, and offering enhanced sensitivity for the high-redshift observations.

D.8.2 Optics Configuration

Figure D-9 shows the SPICA telescope and BASS optical configuration. A fore-optics relay section with a chopper mirror illuminates the pair of spectrographs. Mirror m3 forms a beam-waist and permits the chopper to be located at the image of the SPICA secondary, minimizing chopper-induced spillover. The chopper mirror is curved, saving one mirror and reducing beam aberration and cross-polarization relative to the comparably compact 3-mirror configuration (flat chopper between two curved mirrors). The spectrometer input feedhorns are separated by 5.7 mm, corresponding to 60″ on the sky. The chopper modulates the astronomical source between the two spectrometer bands. Thus, while one spectrometer is coupled to the source, the other is coupled to reference position 60″ away. The modest requirements for variable chopper period (2 s to 10 s) and duty cycle (>90%) do not significantly drive the chopper mirror design. The half-power beamwidth (HPBW) is 19″ at the longest wavelength, and the chopper repeatability is 3″.

D.8.3 Waveguide Grating Approach

A major problem with conventional grating spectrometers is the large size when scaled to far-IR wavelengths. Spectrometer size scales as the product of wavelength and resolving power, thus the volume scales as the cube of this length scale. Conventional spectrometers typically use planar gratings and multiple collimating and focusing optics, making the size of the spectrometer much larger than the grating itself. The problem is exacerbated when the requirement of large instantaneous bandwidth is included. We have developed and tested a new approach that overcomes these limitations for BASS.

The WaFIRS system couples a single spatial mode through a feedhorn, propagates the radiation in a parallel plate, and uses a custom-machined (not ruled) curved grating. Radiation is focused onto an arc, which accommodates the

Table D-5. BASS Spectrograph Modules

BASS: R=300, 2-beam system, 320 NTD-sensed bolometers										
WaFIRs Modules: 2 modules, 1.5 kg mass offset per module										
Band	**λ_{min} μm**	**λ_{max} μm**	**R**	**L cm**	**spac μm**	**flt tol μm**	**H cm**	**2-d tol μm**	**M_{scale} kg (1 mod)**	**M_{tot} kg**
A	132	211	300	7.3	495	46	1.0	13	0.05	1.55
B	211	339	300	11.7	795	75	1.2	21	0.07	1.57

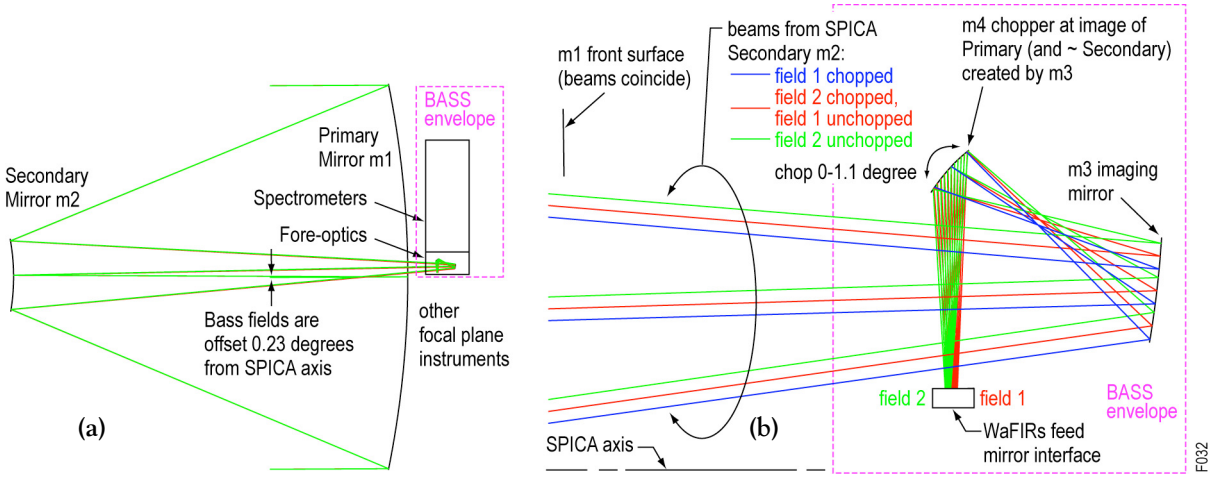

Figure D-9. *BASS optics layout: (a) Two sub-assemblies in the focal plane of the SPICA telescope and (b) detail of fore-optics.*

1-D detector array (see Bradford et al. 2003). Relative to conventional ruled gratings, the machined grating offers the potential to minimize aberrations and thus provides greater flexibility in optical design. It allowing a faster (more compact) system and does not require additional focusing elements beyond the grating itself. Further, the two-dimensional geometry dramatically reduces the system mass and therefore cost for a single beam, and presents the possibility for stacking multiple modules. Our prototype instrument Z-Spec (**Figure D-10**) operates at the Caltech Submillimeter Observatory atop Mauna Kea. Z-Spec provides instantaneous coverage from 190–310 GHz, at a resolving power of 250–400, with sensitivities close to the background limit. The design can be simply scaled with wavelength and the resolving power ($\propto N_{facets}$), and this forms the basis of BASS. The BASS instrument configuration is shown in **Figure D-11**.

D.8.4 BASS Detectors

Perhaps the most demanding technical aspect of BASS is the long-wavelength detectors and the associated readouts. For wavelengths beyond the 38 μm silicon BIB cutoff, sensitive large-format detector arrays which can be built for flight remain a non-trivial technical hurdle. Bulk germanium photoconductors have been used to 200 μm (e.g. on Spitzer and previous missions), but devices are large and thus susceptible to cosmic-ray spikes, exhibit a variety of non-linear behaviors, require mechanical stressing, and do not provide complete wavelength coverage. Bolometer development in the U.S. has been supported by NASA for many decades, particularly for studies of the CMB and for X-ray and far-infrared/sub-mm astronomy. This investment has achieved especially notable scientific successes in COBE and BOOMERANG. Low-temperature bolometers developed by NASA-JPL are now ready for launch on the Planck-HFI and the Herschel-SPIRE instruments in 2008.

The BASS instrument will use low-background neutron transmutation doped (NTD) germanium bolometers operating from a base temperature of 50 mK. Arrays of very similar NTD Ge bolometers operating at 300 mK have been space-qualified by JPL for the SPIRE instrument on Herschel. Single-element NTD Ge bolometers operating at 100 mK have been space-qualified by JPL for the High Frequency Instrument on Planck. Herschel and Planck are scheduled for a joint launch in 2008.

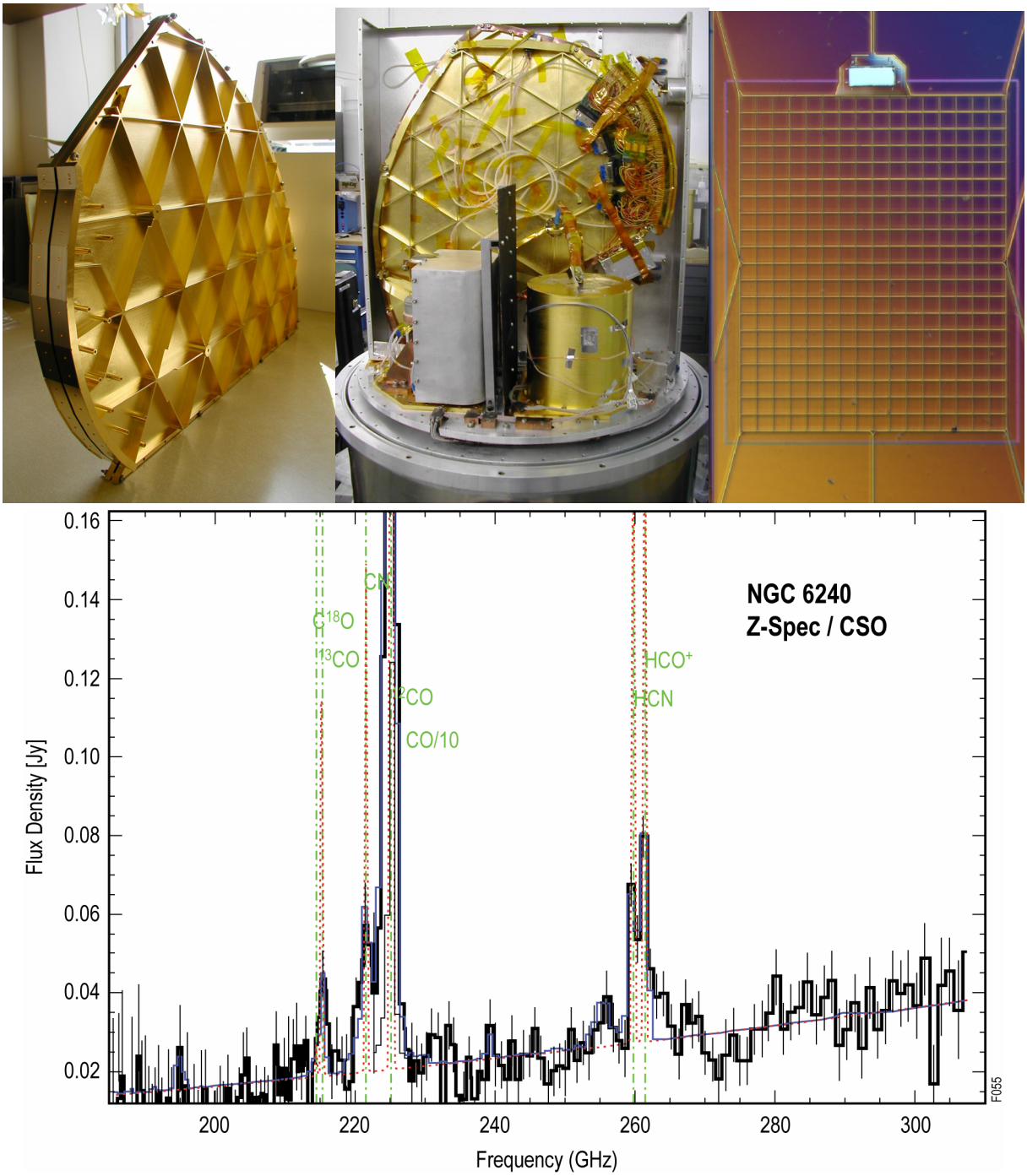

Figure D-10. *Z-Spec, the WaFIRS waveguide spectrometer prototype for 1 mm wavelength [upper left], and integrated with its cryostat and 50 mK refrigeration system [upper middle]. Z-Spec provides R~300 from 190 to 310 GHz (1-1.6mm) with a grating which is 55 cm in its longest dimension. In the right picture, the light enters the parallel plate section via a feedhorn in the upper right, and illuminates the curved 480-facet grating on the left. The 160 bolometers couple to the parallel plate through curved waveguide feeds to both the front and back of the structure. Bolometers are individually mounted, a close up view of the 2.5 mm by 1.6 mm absorber region with NTD thermistor chip is shown in the upper right. This instrument is operating at the Caltech Submillimeter Observatory with 100% detector yield and near-background-limited performance there, as the spectrum below shows. The WaFIRS modules size scales as $\lambda \times R$, and BASS bands A and B are simply scaled from Z-Spec.*

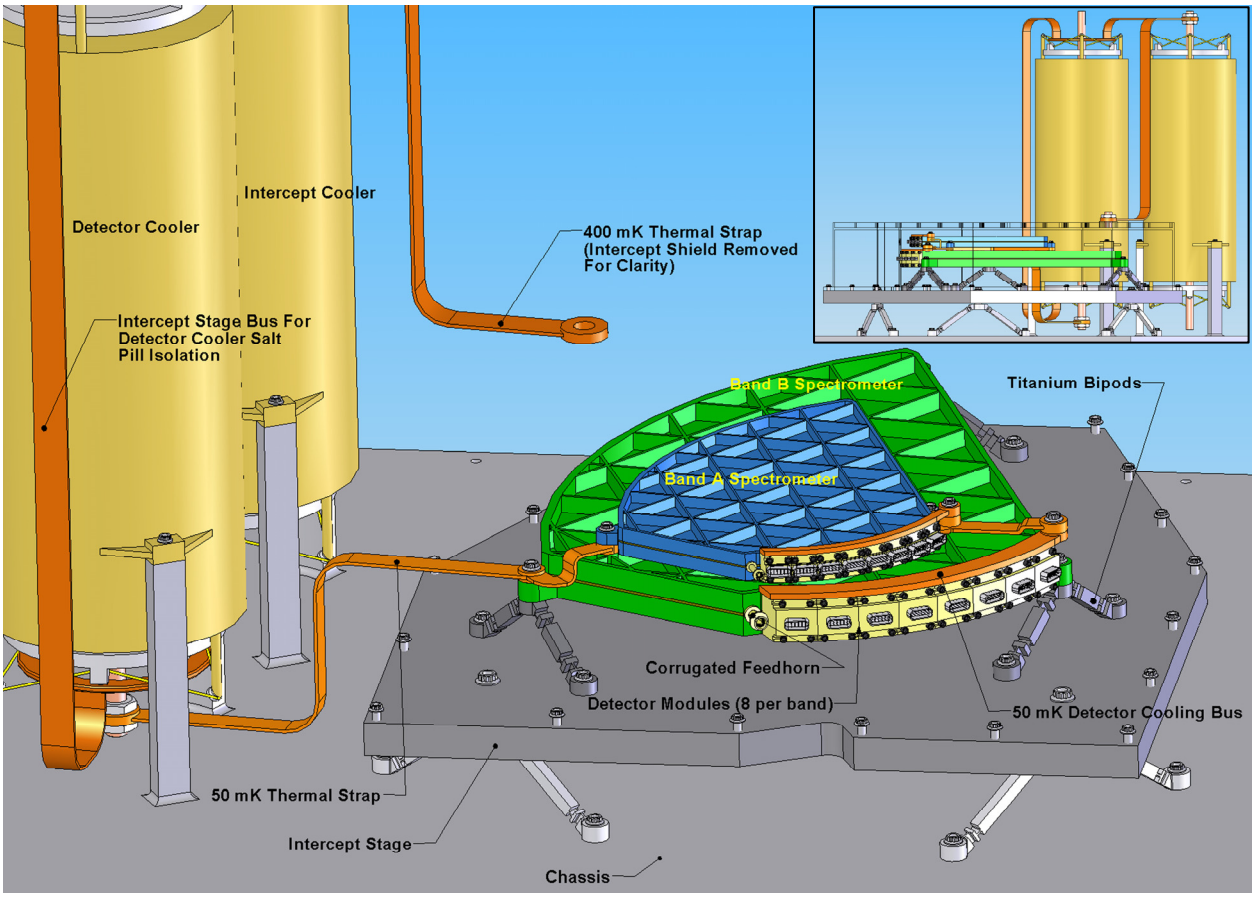

Figure D-11. *BASS layout (schematic). Band A and B waveguide spectrometers have size scaled with wavelength. The input feedhorns are separated by 5.7 mm, corresponding to the 60 arcsecond chop throw. The detector cold stage (50 mK) and the intercept stage (~400–500 mK) are each cooled with an ADR. The intercept shield is removed for clarity, but is shown in elevation view in upper right).*

Table D-6. BASS Detector Loadings, Requirements, and Design Values

Loading			Requirements						Design Values				
Band	P_{opt} aW	NEP_{phot} aW $Hz^{-1/2}$	NEP aW $Hz^{-1/2}$	τ ms	η_{abs}	1/f knee Hz	format	N_{types}	NEP aW $Hz^{-1/2}$	τ ms	G_0 pW/K	C_0 fJ/K	V_n (amp) nV $Hz^{-1/2}$
A	1.3	0.039	0.5	300	0.8	0.1	8×(1×20)	1, 2	0.25	130	0.9	30	10
B	0.6	0.044	0.5	300	0.8	0.1	8×(1×20)	1, 2	0.25	130	0.9	30	10

NOTE: N_{types} is the number of different types (bolometers, back-shorts) for each band.

The requirements for the BASS bolometers, which carry a factor of 2 margin in detector NEP and heat capacity, are described in **Table D-6**. Sensitivity margin will be allocated to systems issues during the development of the instrument. While the detectors have slow response times of 130–300 ms, this does not incur any sensitivity penalty with stable readout electronics that have already been developed and tested. The SPIRE instrument already demonstrates 10 times better stability than the BASS requirement of a 100 mHz 1/f knee. The bolometers have a high degree of dynamic range, giving $NEP_{det} = NEP_{photon}$ under an optical power ~100,000 times larger than the design loading.

The BASS bolometers will be thermally isolated on silicon nitride support members, and read out with superconducting Niobium leads. The devices will be optically coupled through bare absorbers and a tuned backshort in linear arrays of 20 devices. Each spectrometer assembly will have 8 linear arrays with two backshort

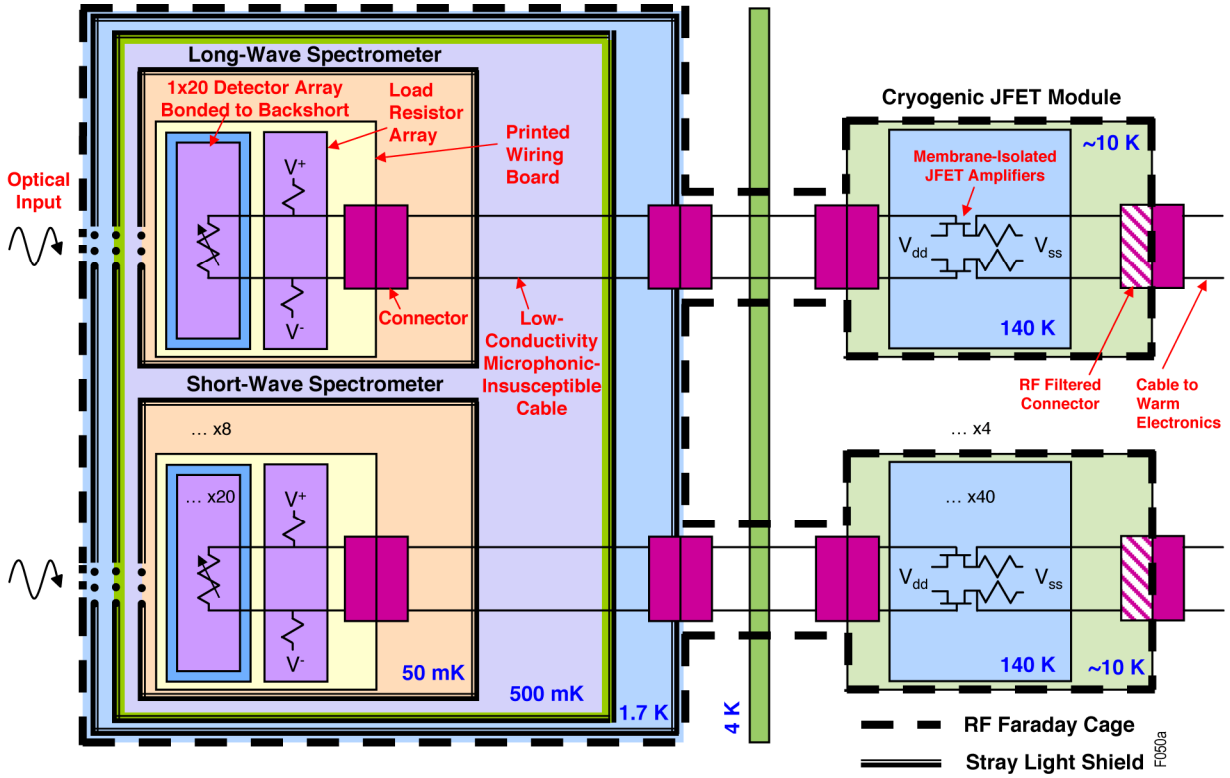

Figure D-12. *A block diagram of the BASS detector and readout chain. Detectors are assembled into modules of 1x20 linear bolometers arrays bonded to backshorts (2 types per spectrometer) and mounted with biasing load resistors onto a printed circuit board. BASS requires 16 detector modules in total, 8 per spectrometer. Pairs of 2x20 channels are read out using cryogenic JFET power amplifiers developed for Herschel/SPIRE. BASS incorporates proven defenses against systems issues developed for Herschel, Planck, and Z-Spec. The detectors are enclosed in a cryogenic Faraday cage to reduce susceptibility to EMI/EMC. Following SPIRE, every wire into the Faraday cage is RF filtered. The readout is based on a balanced AC-biased differential design to minimize response to common-mode signals. Following Z-Spec, three levels of shielding at 50 mK, 500 mK and 1.7 K are used to defeat stray light. The detectors view the instrument space only through the 50 mK spectrometer, which defines a narrow spectral band and a single electromagnetic mode for minimal coupling to stray photons from the instrument. Microphonic response is mitigated by using the carbon-jacketed microphonically insusceptible low-conductivity cabling developed for the Planck 100 mK bolometers.*

distances. The optical coupling scheme follows the same design used on the Z-Spec spectrometer. A single pixel on Z-Spec is shown in **Figure D-10**.

The detectors will be assembled into focal plane panels using a process closely following that used in the manufacture of the SPIRE bolometer arrays. JPL developed 10 flight arrays for SPIRE, with 5 different array designs. These arrays exceeded all of the stringent performance requirements of the SPIRE instrument, and in some cases surpasses the performance goals. Laboratory tests of the SPIRE arrays indicate an average optical efficiency of 73 %, a detector NEP sub-dominant to the photon NEP as designed to match the expected flight loading, a 1/f knee below 30 mHz, and a total yield of 98.5% including both non-functioning and noisy detectors. A block diagram of detector module is shown in **Figure D-12**, and an open view of a SPIRE detector assembly showing the mounted array, backshort, and load resistors is shown in **Figure D-13**.

The 20-element BASS detector sub-arrays will be fabricated on 4″ wafers, and screened for functionality at room temperature. Each array will be hybridized to a backshort wafer and mounted in a detector readout module. The readout module will have lithographed bias resistors and electrical connection to low-

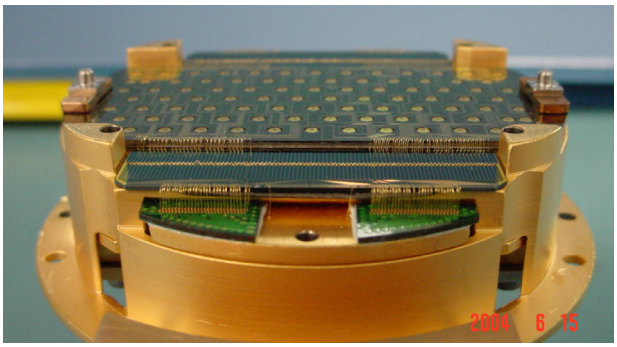

Figure D-13. *Focal plane assembly of the SPIRE instrument incorporating NTD Ge bolometer array, micro-machined backshort array, biasing load resistors, and wirebonds to low thermal conductivity kapton cables.*

conductivity cables for readout. The hybridization process will be carried out in JPL's electronics packaging laboratory. Eight readout modules will be mated to each spectrometer and delivered to the array testbed.

In the development phase we plan to adapt the SPIRE/Planck NTD process to the low-background requirements of BASS, which will be designed to have 2 orders of magnitude lower NEP than SPIRE. This will require a lower operating temperature, lower thermal conductance, and lower heat capacity. The lower operating temperature will require a higher NTD Ge doping level than that used for SPIRE. Resistance as a function of temperature will be measured for NTD Ge samples to determine the optimum doping for 50 mK operation. The thermal conductance of the SPIRE bolometers was selected by the Au thermistor leads; for BASS the Au will be replaced with superconducting Nb so that the limiting factor will be the conductance of the Si_3N_4 absorber legs. We do not anticipate difficulty in achieving the required thermal isolation: bolometers using Nb/Si_3N_4 leads have already demonstrated thermal isolation 100 times lower than the BASS design value. We will adapt the SPIRE membrane etch and release process to be compatible with Nb leads.

Finally we plan a series of tests to reduce the heat capacity of the bolometers, which is currently limiting the detector NEP due to the speed of response requirement (**Table D-6**). However, the required speed of response can be met with the existing SPIRE NTD Ge chip and contacts technology, conservatively scaling the achieved heat capacity of the SPIRE bolometers. At the end of the advanced development phase, the bolometers developed will undergo component thermal cycling and accelerated aging testing to verify readiness for the flight build phase.

D.8.5 Cyrogenics Cooler Subsystem

The BASS cryogenic subsystem consists of a 2-stage adiabatic demagnetization refrigerator (ADR) that cools both the detector system to 50mK and also an intercept stage. The intercept stage serves as thermal radiation and stray light shield and dramatically reduces the conducted heat loads to the detector stage. The ADR, opto-mechanical structures, intercept shield and detector subsystem are mounted inside a chassis cooled by the SPICA facility cooler to 1.7 K. A high-heat-capacity thermal ballast is mounted in the chassis to minimize thermal disturbances created by the ADR on the other SPICA instruments. Other than the optical access port, the chassis is light tight to prevent direct viewing of high temperature (>4K) thermal radiation sources on SPICA, and to control stray light from the telescope. The chassis is mounted to the 4.5-K optical bench using low-thermal-conductance standoffs.

The cooling cycle for the BASS ADR system, is as follows (refer **Figure D-14**). A pair of ^{3}He filled gas gap switches are turned to the ON state to conduct heat to the 1.7 K cold stage.as the magnet currents are ramped up. After the magnets achieve full field, 20 kG and the cold stages equilibrate at 1.7 K, the heat switches are turned OFF and the magnets are ramped down. The initial ramp down causes rapid cooling of the intercept stage to ~500 mK and the detector stage to 50 mK. Once at temperature, the ramp down rate of the current for each ADR stage is reduced and adjusted on several second intervals to maintain the fixed operating temperatures. This cycle is repeated every 1–2 days at a duty cycle of ~90%. Temperature stability of 1–10 μK/rt Hz at the chop frequency ~0.5 Hz and drift rates <3 mK/hr are required to eliminate contributions to detector noise and maintain calibration accuracy. This presents no problem since stability 1–<0.1 μK/rt Hz at frequencies f>0.01 Hz and drift rates ~2–3 μK/hr were easily achieved for the Planck 100 mK focal plane, a bolometric focal plane similar to BASS.

An ADR, similar in design to the BASS ADR, achieved 60 mK in space on 7/27/05 on

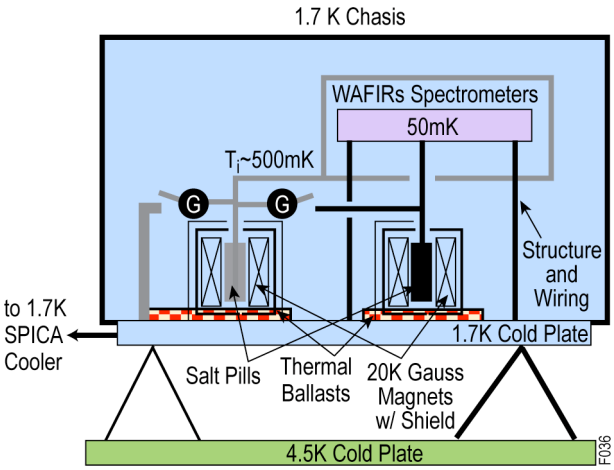

Figure D-14. *BASS Cryogenic subsystem. One stage of the ADR cools the intercept shield to ~500 mK. The second stage cools the detectors and WAFIRs spectrometers to 50 mK. Both ADR stages consist of a salt pill, thermal straps, and a superconducting electromagnet with paramagnetic shield. The ^{3}He filled gas gap heat switches indicated as black dots with a white "G". A high heat capacity thermal ballast is located at the base of the magnets and the heat strap to the 1.7 K cooler to attenuate high heat loads during magnet ramp up.*

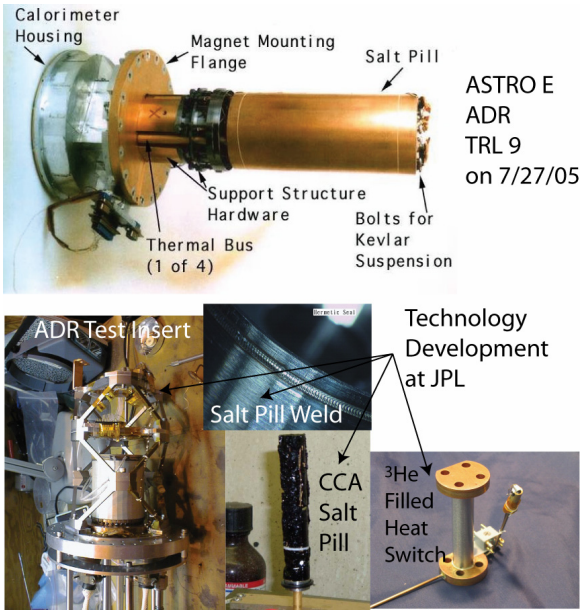

Figure D-15. *ADR technology status. See also Appendix I-11.*

Astro E II. The ADR for Astro E I was never operated due to rocket failure on launch. JPL has invested internal research money to developing components necessary for a space qualified ADR as shown in **Figure D-15**.

The main improvement with the BASS ADR is that two ADR stages are employed to dramatically improve hold time and reduce mass. Functionally, the ADRs for each stage are identical. They differ only in size as dictated by system optimization. However, they could be made identically with a penalty of either 10–20% increase in mass or decrease in cold time. The temperature (50 mK) and heat loads (~2 μW at 50 mK) are typical of sub-Kelvin coolers for ground based instruments. Many of these instruments, for example Z-Spec, are fielded at remote telescopes and cooled by ADRs.

D.9 Core Science Deliverables

We anticipate that the observations for our core program can be carried out within the first year of SPICA observations, or at least be well underway so that analysis can begin (1000 hours of observing is 12% of a year). After the core program, the BASS instrument will be available to SPICA (though this proposal does not include support of BASS during this period).

The science deliverables will be calibrated spectra of the 500 galaxies described in Section D, published in articles and available to the community. The labor will be provided by the PI, 2–3 post doctoral scholars, and the Co-Is. We recognize that our analyses will not likely tap the full potential of the rich dataset. Our emphasis will be on producing calibrated spectra that can be used by the worldwide community, and we anticipate survey articles that will support the further use of the data. The data will be made available in FITS format as well as in raw-product form on a publicly-available website no later than 18 months after receipt of data products from JAXA. We will strive to make them available sooner. The data will also be in a form accessible to existing databases and archives (e.g. NED, IRSA).

To produce these spectra, we will generate a pipeline based on examination of the first 20-40 spectra obtained early in the core science period. Based on experience of the PI and instrument scientist, and the maturity of the NTD bolometer technology, it is anticipated that these basic science products will be calibrated to 10%, absolutely and from channel to channel across the spectrum. This level of calibration is suitable for the bulk of the astrophysics outlined in Sections D.2–D.6. **We have budgeted**

$3.4M (FY08$) for the science team in Phases E and F to carry out this reduction and analysis. This will support the PI, the postdocs, and the Co-Is (part-time) unless indicated in Table D-7.

D.10 Minimum Mission

BASS is optimized for the SMEX MoO cost envelope, yet carries sufficient margin to ensure success within this envelope. Nevertheless, should cost and schedule be threatened, our descope plan is presented in Section F.3, which leads to the minimum mission: a single-band (Band B) spectrometer which uses drift scanning rather than the chopping mirror. In addition to the wavelength coverage reduction, the survey speed would be impacted by the loss of the chopper. However, some of the basic science topics could still be addressed, such as the [CII] surveying (Section D.4.2) which has substantial margin in the baseline BASS instrument.

D.11 Science and Engineering Team

Each member of the BASS science team is selected to perform specific duties, though most are broad experienced scientists who can advise on the overall scope of the project. Team members and their roles and qualifications are summarized in **Table D-7**. In addition to more frequency subgroup interactions, the entire team will interact by bi-monthly telecons and semi-annual working meetings in Pasadena.

We can't wait to get started working with the SPICA team and developing the BASS instrument!

Table D-7. BASS Science Team—Roles and Responsibilities

Science Team Member	Role and Responsibility	Capabilities and Experience
Matt Bradford	PI (JPL)—Carries overall responsibility for all the BASS activities and will be directly involved in all aspects. Will ensure coordination between individuals and Science Team sub-groups.	12 years experience in instrumentation for far-IR–mm wave astrophysics, led the development and commissioning of SPIFI and Z-Spec, two novel background-limited bolometer-based spectrometers for Mauna Kea observatories.
James Bock	Co-I (JPL)—BASS Instrument Scientist—will take much of the responsibility for the instrument development, including interface and requirements definition, scheduling, interacting with QA. Will provide oversight on the BASS detector fabrication tasks. Will serve as PI in the absence of Bradford.	16 years experience, with key roles in scientific and flight programs. PI of the U.S. involvement in Herschel SPIRE (bolometric detectors), and plays critical roles in several sub- orbital microwave and near-IR background experiments.
Alfred Nash	(JPL) Project Manager—day-to-day instrument management. Responsible for cost and schedule management.	14 years experience with flight hardware and instrument development. 10 years experience with instrument management. Managed JPL build of Planck sorption 20 K cooler recently delivered to ESA.
Timothy Koch	(JPL) System Engineering Manager (JPL)—develops technical requirements, coordinates, and manages system-level technical resources.	10 years experience in flight hardware and instrument development plus 7 years experience in balloon-borne radio astronomy payloads.
Warren Holmes	Co-I (JPL)—will lead the development and in-flight operation of the BASS sub-Kelvin refrigerator, and be responsible for the definition of the thermal interfaces between BASS and SPICA.	20 years of experience in low-temperature physics, with an emphasis on refrigerators and bolometer instrumentation. Recently led the testing and qualification of the 100 mK detector arrays delivered by JPL to ESA for Planck HFI.
Hideo Matsuhara	Co-I (ISAS/JAXA)—will be the liaison between the SPICA team and the BASS instrument team. Will ensure that the interfaces are properly communicated between the SPICA mission team and the BASS team. Will participate in scientific analysis	20 years experience in space astronomy, instrumentation, and cryogenics. Akari project scientist. Requires no BASS support.
Bradford, Bock and Holmes will provide scientific oversight on the hardware phases and are funded throughout the project. Together with Nash, Koch, and Matsuhara, they will be responsible for the instrument development, integration with SPICA, and performance in flight.		

Science Team Member	Role and Responsibility	Capabilities and Experience
Lee Armus	Co-I (IPAC)—will lead the development of a pipeline for the BASS data during the in-orbit checkout period at the end of Phase E. Will participate in scientific analysis.	Leading the Instrument Support Team for the IRS at the Spitzer Science Center (SSC). Expert in studies of starburst and luminous infrared galaxies.
George Helou	Co-I (IPAC)—will be responsible for science data interfaces with JAXA, archiving the BASS data at IPAC for public access after proprietary period. Will participate in scientific analysis.	Director of Infrared Processing and Analysis Center (IPAC), and Deputy Director of the SSC. Expert in the spectroscopic study of normal galaxies.
J. D. Smith	Co-I (U. Toledo)—will develop software for the reduction and analysis of the BASS data. Will participate in scientific analysis.	Has written and released similar software for the Spitzer IRS that is widely used by the astronomical community. Expert in spectroscopy of dust features in normal galaxies.
In addition to their scientific roles, Armus, Helou, and Smith will coordinate the data pipelining and develop basic software tools for the BASS data. Once science-quality data are in hand, all members of the science team will participate in the analysis and publication. Our budget includes two postdoctoral scholars for two years each in phases E, F, and it is anticipated that these younger scientists will play a major role in the analysis well as Bradford and the team members below. To advise in the analysis and publication of the data, our team includes experts in all areas relevant to the BASS science program. Our budget includes funding for all science personnel which require it in Phases D,E,F.		
Scott Chapman	Co-I (Cambridge)—will provide modeling support for BASS distant galaxy sample selection.	Expert,in high-redshift dusty galaxy populations has developed models for high-redshift dusty galaxy populations. Requires no BASS support.
Uma Gorti	Co-I (Ames)—will guide the interpretation of the BASS observations of disks.	Expert, has developed models of far-IR line emission of protoplanetary disks.
Martin Harwit	Co-I (Cornell)—will consult on far-IR cooling lines of molecular gas, and development of an international mission.	Expert in far-IR molecular cooling lines, has experience in international mission development and operation through ISO and Herschel.
Daniel Lester	Co-I (Univ. Texas)—will guide the interpretation of elemental abundances from N, O, and C spectroscopic measurements. Will serve as liaison with SAFIR / CALISTO study team	Has made similar measurements in Galactic regions and nearby galaxies with the Kuiper Airborne Observatory. PI of SAFIR and CALISTO mission concept studies.
Takao Nakagawa	Co-I (ISAS/JAXA)— SPICA PI. Will work with the BASS team during the formulation and development phase, and he has final authority to approve the role of BASS within SPICA, including scientific capability and interface requirements.	20 years experience in far-IR instrumentation and astronomy from space-borne and balloon platforms. Played major role in JAXA Akari mission. Requires no BASS support.
Matt Malkan	Co-I (UCLA)—will guide interpretation of diagnostics of active galactic nuclei (AGN).	Expert in the study of AGN, both obscured and un-obscured. Requires no BASS support.
George Rieke	Co-I (Arizona)—will advise on the far-IR scientific and technical results with Spitzer MIPS, will provide a liaison with the mid-IR instrument on JWST (MIRI).	Spitzer MIPS PI, leading large guaranteed-time programs. Science lead for MIRI. Requires no BASS support.
Gordon Stacey	Co-I (Cornell)—will guide the analysis of far-IR fine-structure line cooling of the interstellar medium.	Over 27 years experience in far-IR spectroscopy and spectroscopic instrumentation, Authored over 100 refereed articles on the subject. Requires no BASS support.
Michael Werner	Co-I (JPL)—will consult on strategies for AGN identification and study, will consult on requirements definition and development issues.	Spitzer Project Scientist, JPL Astronomy and Physics Chief Scientist. Requires no BASS support.

I-12. ACRONYMS LIST

A&A	Astronomy & Astrophysics
ADP	advanced development phase
ADR	adiabatic demagnetization refrigerator
AGN	active galactic nuclei
AIDS	Assembly Instruction Data Sheets
ALMA	Atacama Large Millimeter/submillimeter Array
AO	Announcement of Opportunity
ApJ	Astrophysical Journal
ApJS	Astrophysical Journal Supplement Series
Ap&SS	Astrophysics and Space Sciences
ATLO	Assemble Test and Launch Operations
AURA	Association of Universities for Research in Astronomy
BASS	Bolometer Array Survey Spectrograph
BB	brassboard
BCE	bench checkout equipment
BDA	Bolometric Detector Assembly
BIB	Blocked Impurity Band
BLISS	Background-limited Infrared-submillimeter Spectrograph
BoDAC	Bolometric Detector Assembly Cryostat
BOOMERANG	Balloon Observations of Millimetric Extragalactic Radiation and Geophysics
BPM	Baseband Processor Module
CAE	computer-aided engineering
CALISTO	Cryogenic Aperture Large Infrared Submillimeter Telescope Observatory
CBE	Current Best Estimate
CCAT	Cornell-Caltech Atacama Telescope
CDR	Critical Design Review
CIB	cosmic infrared background
CM	Configuration Management
CMB	cosmic microwave background
COBE	Cosmic Background Explorer
CogEs	Cognizant Engineers
Co-I	Co-investigator
COTS	Commercial Off The Shelf
C/S	Cost/Schedule
CTM	Contract Technical Manager
DC	direct current
DDP	Downlink Data Processor
DEA	Digital Electronics Unit
DIRBE	Diffuse Infrared Background Experiment (COBE)
DRCU	Detector Readout and Control Unit
DROE	Detector Readout Electronics
DSN	Deep Space Network

EAR	Export Administration Regulations
ECR	engineering change requests
EEE	Electrical, Electronic and Electromechanical (parts)
EEPROM	Electrically Erasable Programmable Read-Only Memory
EGSE	Electronics Ground Support Equipment
EIM	Electrical Interface Model
EMC	Electromagnetic Ct
EMI	Electromagnetic In
E/PO	Education and Public Outreach
ESA	European Space Agency
ESI	European SPICA Instrument
EVM	Earned Value Management
FAR	Federal Acquisition Regulation
FDP	Flight Development Phase
FIR	Far Infrared
FITS	Flexible Image Transport System
FM	Flight Model
FMECA	Failure Modes, Effects and Criticality Analysis
FPGA	Field Programmable Gate Array
FPI	Focal Plane Instrument (SPICA)
FSW	Flight Software
FTE	Full-time Equivalent
FTS	Fourier-transform spectrometer
FVRR	flight validation readiness review
GDS	Ground Data System
GIDEP	Government Industry Data Exchange Program
GPMC	Governing Program Management Council
GSE	Ground Support Equipment
GSRP	Graduate Student Research Program
GY	gigayear (= 1 billion years)
HIFI	Heterodyne Instrument for the Far-Infrared
HFI	High Frequency Instrument
HK	Housekeeper
HKT	House Keeping Telemetry
HPBW	Half Power Beamwidth
HQA	Hardware Quality Assurance
HRCR	Hardware Review and Certification Record
IC	Instrument Controller
ICA	Independent Cost Assessment
ICD	interface control document
IFTS	imaging Fourier-transform spectrometer
IGDS	Instrument Ground Data System
II	Instrument Interface

IMF	Initial Mass Function (stellar)
IP	Instrument Power
IPAC	Infrared Processing and Analysis Center
IPM	Instrument Project Manager
IR	Infrared
IRAS	Infrared Astronomical Satellite
IRS	Infrared spectrograph (Spitzer)
IS	instrument scientist
ISAS	Institute of Space and Astronautical Science (JAXA)
ISE	Instrument System Engineer
ISM	Interstellar Medium
ISO	Infrared Space Observatory (ESA)
I&T	Integration and Test
ITAR	International Traffic in Arms Regulations
JAXA	Japanese Aerospace Exploration Agency
JCMT	James Clerk Maxwell Telescope
JFET	junction gate field-effect transistor
JHU	Johns Hopkins University
JPL	Jet Propulsion Laboratory
JWST	James Webb Space Telescope
KASI	Korean Astronomy and Space Science Institute
LIRGs	luminous infrared galaxies
LOM	life of mission
LSCI	Light and Spectroscopy Concept Inventory
LWS	Long-wavelength Spectrometer
M^3	Moon Mineralogy Mapper
M^3 SCIF	Moon Mineralogy Mapper Instrument Spacecraft Interface
MAMBO	Max-Planck Millimeter Bolometer array
MDL	Micro Devices Laboratory
MDR	Mission Definition Review
MIL	Military Specification
MIPL	Multi-mission Image Processing Laboratory
MIPS	multi-band imaging photometer
MIRI	Mid-Infrared Instrument (JWST)
MNRAS	Monthly Notices of the Royal Astronomical Society
MoO	Mission of Opportunity
MOS	Mission Operations System
MRO	Mars Reconnaissance Orbiter
MSL	Mars Science Laboratory
MSRD	mission/system requirements document
MTO	Marts Telecom Orbiter
NASA	National Aeronautics and Space Administration
Natur	Nature

NED	NASA/IPAC Extragalactic Database
NEP	Noise Equivalent Power
NIAT	NASA Integrated Action Team
NICM	NASA Instrument Subsystem Cost Model
NTD	Neutron Transmutation Doped
OEC	Office of Export Compliance
PAH	Polycyclic Aromatic Hydrocarbon
PAIP	Performance Assurance Implementation Plan
PAM	Product Assurance Manager
PC	Payload Controller
PCB	printed circuit board
PCU	Power Conditioning Unit
PDMS	Product Data Management System
PDR	photo-dissociated region
PFM	Proto-Flight Models
PFM	Proto-Flight Model
PIAA	phase-induced amplitude apodisation
PI	Principal Investigator
PO	Purchase Orders
PROM	Programmable Read Only Memory
PSF	point spread function
PSR	pre-ship review
PWB	Printed Wiring Board
QA	quality assurance
QSO	Quasi-stellar Object (Quasar)
RAM	Random Access Memory
RF	Radio Frequency
RFI	Radio Frequency Interference
RFP	Request for Proposal
RID	Review Item Discrepancy
RT	remote terminal
SAFIR	Single Aperture FIR observatory
SCIF	Spacecraft Interface
SCUBA	Submillimetre Common-User Bolometer Array (JCMT)
SDB	Small Disadvantaged Business
SDR	system definition review
SED	spectral energy distribution
SEE	Single-Event Effects
SEIP	System Engineering Implementation Plan
SINGS	Spitzer Infrared Nearby Galaxy Survey
SMA	Safety and Mission Assurance
SMD	Science Mission Directorate
SMEX	Small Explorers

SMGs	Sub-millimeter Galaxies
SOFIA	Stratospheric Observatory for Infrared Astronomy
SOW	Statement of Work
SPICA	Space Infrared Telescope for Cosmology and Astrophysics
SPIE	Proceedings of the Society of Photo-Optical and Instrumentation Engineers (Proc. SPIE for short)
SPIFI	South Pole Imaging Fabry-Perot Interferometer
SPIRE	Spectral and Photometric Imaging Receiver
SPIRIT	Space Infrared Interferometric Telescope
SRR	System Requirements Review
SS	subsystem
STD	standard
STM	Structural Thermal Model
STScI	Space Telescope Science Institute
TAA	Technical Assistance Agreement
TDS	Terminal Descent Subsystem
TES	transition-edge-sensed
TMC	Technical, Management, and Cost
TRL	Technology Readiness Level
UofA	University of Arizona
ULIRGs	ultra-luminous galaxies
UV	ultraviolet
VLA	Very Large Array
WaFIRS	Waveguide Far-IR Spectrometer
WBS	Work Breakdown Structure
XDR	X-ray dominated region
ZSPEC	(Broadband FIR Spectrometer, Mauna Kea)

I-13. REFERENCES

Agnor, C.B., and W.R. Ward. 2002. Damping of terrestrial-planet eccentricities by density-wave interactions with a remnant gas disk. *ApJ* 567:579A.

Arendt, R.G., N. Odegard, J.L. Weiland, T.J. Sodroski, M.G. Hauser, E. Dwek, T. Kelsall, S.H. Moseley, R.F. Silverberg, D. Leisawitz, and 3 co-authors. 1998. The COBE diffuse infrared background experiment search for the cosmic infrared background. III. Separation of galactic emission from the infrared sky brightness. *ApJ* 508:74A.

Barder, P., Becher, and Slater. 2006. Development and validation of the Light and Spectroscopy Concept Inventory. *Astronomy Education Review* 5(2). http://aer.noao.edu/cgi-bin/

Bell, E.F., T. Naab, D.H. McIntosh, R.S. Somerville, J.A.R. Caldwell, M. Barden, C. Wolf, Christian, H.W. Rix, S.V. Beckwith, A. Borch, and 9 co-authors. 2006. Dry mergers in GEMS: The dynamical evolution of massive early-type galaxies. *ApJ* 640:241B.

Boss, Alan P. 2002. Rapid formation of outer giant planets by disk instability. *ApJ* 576:462B.

Bradford, C.M., B.J. Naylor, J. Zmuidzinas, J.J. Bock, J. Gromke, H. Nguyen, M. Dragovan, M. Yun, L. Earle, J. Glenn, and 3 co-authors. 2003. WaFIRS: a waveguide far-IR spectrometer: enabling spectroscopy of high-*z* galaxies in the far-IR and submillimeter. *SPIE* 4850:1137B.

Bradford, C.M., P.A.R. Ade, J.E. Aguirre, J.J. Bock, M. Dragovan, L. Duband, L. Earle, J. Glenn, H. Matsuhara, B.J. Naylor, and 3 co-authors. 2004. Z-Spec: a broadband millimeter-wave grating spectrometer: design, construction, and first cryogenic measurements. *SPIE* 5498:B.

Bradford, C.M., T. Nikola, G.J. Stacey, A.D. Bolatto, J.M. Jackson, M.L. Savage, J.A. Davidson, and S.J. Higdon. 2003. CO (J=7-->6) observations of NGC 253: Cosmic-ray-heated warm molecular gas. *ApJ* 586:891B.

Caputi, K.I., G. Lagache, L. Yan, H. Dole, and N. Bavouzet et al. 2007. The infrared luminosity function of galaxies at Redshifts $z=1$ and $z\sim2$ in the GOODS Fields. *ApJ* 660:97–116.

Chapman, S.C., A.W. Blain, I. Smail, and R.J. Ivison. 2005. A redshift survey of the submillimeter galaxy population. *ApJ* 622:772–796.

Chapman, S.C., D. Scott, C. Borys, and G.G. Fahlman. 2002. Submillimetre sources in rich cluster fields: source counts, redshift estimates and cooling flow limits. *Monthly Notices of the Royal Astronomical Society* 330(1):92–104.

Chapman, S.C., I. Smail, R. Windhorst, T. Muxlow, and R.J. Ivison. 2004. Evidence for extended, obscured starbursts in submillimeter galaxies. *ApJ* 611:732C.

Chary, R., S. Casertano, M.E. Dickinson, H.C. Ferguson, and P.R.M. Eisenhardt et al. 2004. *ApJ Suppl.* 154:80–86.

Colbert, J.W., M.A. Malkan, P.E. Clegg, P. Cox, J. Fischer, S.D. Lord, M. Luhman, S. Satyapal, H.A. Smith, L. Spinoglio, and 2 co-authors. 1999. ISO LWS Spectroscopy of M82: A unified evolutionary model. *ApJ* 511:721C.

Daddi, E., D.M. Alexander, M. Dickinson, R. Gilli, A. Renzini, D. Elbaz, A. Cimatti, R. Chary, D. Frayer, F.E. Bauer, W.N. Brandt, M. Giavalisco, N.A. Grogin, M. Huynh, J. Kurk, M. Mignoli, G. Morrison, A. Pope, and S. Ravindranath. 2007. Multiwavelength study of massive galaxies at $z\sim2$. II. Widespread compton-thick active galactic nuclei and the concurrent growth of black holes and bulges. *ApJ* 670:173–189.

Daddi, E., M. Dickinson, G. Morrison, R. Chary, and A. Cimatti et al. 2007. Multiwavelength study of massive galaxies at $z\sim2$. I. star formation and galaxy growth. *ApJ* 670:156–172. In press.

Dale, D.A., G. Helou, J.R. Brauher, R.M. Cutri, S. Malhotra, and C.A. Beichman. 2004. [O I] 63 micron emission from high- and low-luminosity active galactic nucleus galaxies. *ApJ* 604:565D.

Davé, R. 2007. The galaxy stellar mass-star formation rate relation: Evidence for an evolving stellar initial mass function? *MNRAS.* Submitted. arXiv:0710.0381.

Dole, H., G. Lagache, J-L Puget, K.I. Caputi, and N. Fernández-Conde et al. 2006. *Astron. Astrophys.* 451:417–429.

Draine, B.T., D.A. Dale, G. Bendo, K.D. Gordon, J.D.T. Smith, L. Armus, C.W. Engelbracht, G. Helou, R.C. Jr. Kennicutt, A. Li, and 10 co-authors. 2007. Dust masses, PAH abundances, and starlight intensities in the SINGS galaxy sample. *ApJ* 663:866D.

Engelbracht, C.W. et al. 2008. *ApJ*. Submitted.

Enya, K., S. Tanaka, T. Nakagawa, H. Kataza, L. Abe, M. Tamura, J. Nishikawa, N. Murakami, K. Fujita, and Y. Itoh. 2006. Development of an MIR coronagraph for the SPICA mission. *SPIE* 6265:626536.

Figer, D.F. 2005. The Formation and Evolution of Massive Young Star Clusters. eds. H.J.G.L.M. Lamers, L.J. Smith, and A. Nota. *ASP Conf. Series* 322:49.

Fischer, J., M.L. Luhman, S. Satyapal, M.A. Greenhouse, G.J. Stacey, C.M. Bradford, S.D. Lord, J.R. Brauher, S.J. Unger, P.E. Clegg, H.A. Smith, G. Melnick, J.W. Colbert, M.A. Malkan, L. Spinoglio, P. Cox, V. Harvey, J.P. Suter, and V. Strelnitski. 1999. ISO FAR-IR spectroscopy of IR-bright galaxies and ULIRGs. *Ap&SS* 266:91F.

Frayer, D.T., M.T. Huynh, R. Chary, M. Dickinson, and D. Elbaz et al. 2006. Spitzer 70 Micron Source Counts in GOODS-North. *ApJ Lett.* 647:L9–12.

Goldader, J.D., G. Meurer, T.M. Heckman, M. Seibert, D.B. Sanders, D. Calzetti, and C.C. Steidel. 2002. Far-infrared galaxies in the far-ultraviolet. *ApJ* 568:651G.

González-Alfonso, E., H.A. Smith, J. Fischer, and J. Cernicharo. 2004. The far-infrared spectrum of Arp 220. *ApJ* 613:247G.

Gorti, U., and D. Hollenbach. 2004. Models of chemistry, thermal balance, and infrared spectra from intermediate-aged disks around G and K stars. *ApJ* 613:424G.

Gorti, U., and D. Hollenbach. 2008. *ApJ.* Submitted.

Hailey-Dunsheath et al. 2008. *ApJ.* Submitted.

Hopkins, A.M., and J.F. Beacom. 2006. On the normalization of the cosmic star formation history. *ApJ* 651:142.

Kaufman, M.J., M.G. Wolfire, D.J. Hollenbach, M.L. Luhman. 1999. Far-infrared and submillimeter emission from galactic and extragalactic photodissociation regions. *ApJ* 527:795K.

Kelsall, T., J.L. Weiland, B.A. Franz, W.T. Reach, R.G. Arendt, E. Dwek, H.T. Freudenreich, M.G. Hauser, S.H. Moseley, N.P. Odegard, and 2 co-authors. 1998. The COBE diffuse infrared background experiment search for the cosmic infrared background. II. Model of the interplanetary dust cloud. *ApJ* 508:44K.

Kominami, J., and S. Ida. 2002. The effect of tidal interaction with a gas disk on formation of terrestrial planets. *Icar* 157:43K.

Kominami, J., and S. Ida. 2004. Formation of terrestrial planets in a dissipating gas disk with Jupiter and Saturn. *Icar* 167:231K.

Kornet, K., P. Bodenheimer, and M. Różyczka. 2002. Models of the formation of the planets in the 47 UMa system. *A&A* 396:977K.

Krolik, J. H., S. Lepp. 1989. The physical state of the obscuring torus in Seyfert galaxies. *ApJ* 347:179K.

Le Floc'h, E., C. Papovich, H. Dole, E. Bell, and G. Lagache et al. 2005. *ApJ* 632:169–190.

Lester, D. F., H.L. Dinerstein, M.W. Werner, D.M. Watson, R. Genzel, and J.W.V. Storey. 1987. Far-infrared measurements of N/O in H II regions - Evidence for enhanced CN process nucleosynthesis in the inner Galaxy. *ApJ* 320:573–585.

Lester, D.F., H.L. Dinerstein, M.W. Werner, D.M. Watson, R. Genzel, and J.W.V. Storey. 1987. Far-infrared measurements of N/O in H II regions - Evidence for enhanced CN process nucleosynthesis in the inner galaxy. *ApJ* 320:573L.

Lotz, J.M., P. Madau, M. Giavalisco, J. Primack, H. Ferguson, and C. Henry. 2006. The rest-frame far-ultraviolet morphologies of star-forming galaxies at $z \sim 1.5$ and 4. *ApJ* 636:592L.

Luhman, M.L., S. Satyapal, J. Fischer, M.G. Wolfire, P. Cox, S.D. Lord, H.A. Smith, G.J. Stacey, and S.J. Unger. 1998. Infrared space observatory measurements of a [C II] 158 micron line deficit in ultraluminous infrared galaxies. *ApJ* 504:11L.

Lutz, D., L. Yan, L. Armus, G. Helou, and L.J. Tacconi et al. 2005. *ApJ. Lett.* 632:L13–16.

Maloney, P.R. 1999. The impact of star formation and active nuclei on the interstellar medium in ultraluminous infrared galaxies. *Ap&SS* 266:207M.

Maloney, P.R., D.J. Hollenbach, and A.G.G.M. Tielens. 1996. X-ray–irradiated molecular gas. I. Physical processes and general results. *ApJ* 466:561M.

Meijerink, R., and M. Spaans. 2005. Diagnostics of irradiated gas in galaxy nuclei. I. A far-ultraviolet and X-ray dominated region code. *A&A* 436:397M.

Moorwood, A.F.M., D. Lutz, E. Oliva, A. Marconi, H. Netzer, R. Genzel, E. Sturm, and T. de Graauw. 1996. 2.5-45μm SWS spectroscopy of the Circinus Galaxy. *A&A* 315L:109M.

Nakagawa, T., and H. Murakami. 2007. *Advances in Space Research* 40:679–683.

Nakagawa, T., K. Enya, M. Hirabayashi, H. Kaneda, T. Kii, Y. Kimura, T. Matsumoto, H. Murakami, M. Murakami, K. Narasaki, M. Narita, A. Ohnishi, S. Tsunematsu, and S. Yoshida. 2007. Flight performance of the AKARI Cryogenic System. *Publications of the Astronomical Society of Japan.* arXiv:0708.1797.

Narasaki, K., S. Tsunematsu, K. Ootsuka, N. Watanabe, T. Matsumoto, and H. Murakami et al. 2004. Development of 1 K-class mechanical cooler for SPICA. *Cryogenics* 44:375–381.

Papovich, C., G. Rudnick, E. Le Floc'h, P.G. van Dokkum, G.H. Rieke, E.N. Taylor, L. Armus, E. Gawiser, J. Huang, D. Marcillac, and M. Franx. 2007. Spitzer mid- to far-infrared flux densities of distant galaxies. *ApJ* 668:45–61.

Papovich, C., H. Dole, E. Egami, E. Le Floc'h, and P.G. Pérez-González et al. 2004. The 24 micron source counts in deep spitzer space telescope surveys. *ApJ Suppl.* 154:70–74.

Pascucci, I., U. Gorti, D. Hollenbach, J. Najita, M.R. Meyer, J.M. Carpenter, L.A. Hillenbrand, G.J. Herczeg, D.L. Padgett, E.E. Mamajek, and 10 co-authors. 2006. Formation and evolution of planetary systems: Upper limits to the gas mass in disks around sun-like stars. *ApJ* 651:1177P.

Pérez-González, P.G., G.H. Rieke, E. Egami, A. Alonso-Herrero, and H. Dole et al. 2005. *ApJ* 630:82–107.

Pope, A., R. Chary, M. Dickinson, and S. Scott. 2006. Infrared spectral energy distributions of submillimetre galaxies. *ASP Conf. Series*. In press.

Reddy, N.A., C.C. Steidel, M. Pettini, K.L. Adelberger, and A.E. Shapley et al. 2007. Multi-wavelength constraints on the cosmic star formation history from spectroscopy: the rest-frame UV, H-alpha, and infrared luminosity functions at redshifts $1.9<z<3.4$. *ApJ.* In press. arXiv0706.4091R.

Rieke, G. H., K. Loken, M.J. Rieke, and P. Tamblyn. 1993. Starburst modeling of M82 - Test case for a biased initial mass function. *ApJ* 412:99.

Rieke, G.H., M.J. Lebofsky, R.I. Thompson, F.J. Low, and A.T. Tokunaga. 1980. The nature of the nuclear sources in M82 and NGC 253. *ApJ* 238:24.

Rigby, J.R., D. Marcillac, E. Egami, G.H. Rieke, J. Richard, J. Kneib, D. Fadda, C.N.A. Willmer, C. Borys, P.P. van der Werf, and 3 co-authors. 2007. Mid-infrared spectroscopy of lensed galaxies at $1<z<3$: The nature of sources near the MIPS confusion limit. 2007. *ApJ.* In press. arXiv0711.1902R.

Rubin, R.H. 1985. Models of H II regions - Heavy element opacity, variation of temperature. *ApJS* 57:349.

Smail, I., R. J. Ivison, A.W. Blain, and J.P. Kneib. 2002. The nature of faint submillimetre-selected galaxies. *MNRAS* 331:495S.

Sturm, E., D. Lutz, A. Verma, H. Netzer, A. Sternberg, A.F.M. Moorwood, E. Oliva, and R. Genzel. 2002. Mid-Infrared line diagnostics of active galaxies. A spectroscopic AGN survey with ISO-SWS. *A&A* 393:821S.

Sugita, H., T. Nakagawa, H. Murakami, A. Okamoto, H. Nagai, M. Murakami, K. Narasaki, M. Hirabayashi, and SPICA Working Group. 2006. *Cryogenics* 46:149–157.

Swinyard, B., T. Nakagawa et al. 2008. SPICA Cosmic Visions Proposal. *Experimental Astronomy.* Submitted. http://sci.esa.int/spica_proposal

Tielens, A.G.G.M., and D. Hollenbach. 1985. Photodissociation regions. I - Basic model. II - A model for the Orion photodissociation region. *ApJ* 291:722T.

Valiante, E., D. Lutz, E. Sturm, R. Genzel, and L.J. Tacconi et al. 2007. *ApJ* 660:1060–1071.

Watson, D.M., C.J. Bohac, C. Hull, W.J. Forrest, E. Furlan, J. Najita, N. Calvet, P. D'Alessio, L. Hartmann, B. Sargent, and 3 co-authors. The development of a protoplanetary disk from its natal envelope. *Nature* 448:1026W.

Weiß, A., D. Downes, R. Neri, F. Walter, C. Henkel, D.J. Wilner, J. Wagg, and T. Wiklind. 2007. Highly-excited CO emission in APM 08279+5255 at $z = 3.9$. *A&A* 467:955W.

Zuckerman, B., T. Forveille, and J.H. Kastner. 1995. Inhibition of giant planet formation by rapid gas depletion around young stars. *Nature* 373:494Z.